SBORNÍK NÁRODNÍHO MUSEA V PRAZE

Volumen XVI. B (1960) No. 3

REDAKTOR ALBERT PILÁT

JAROSLAV JERMAN:

# Paleohistologické nálezy v riss-würmských travertinech z naleziště Hrádok-Gánovce u Popradu (Československo)

# Paleohistological researches in Riss-Würm travertines in the area Hrádok-Gánovce near Poprad (Czechoslovakia)

(English text pag. 132)

(Předloženo 11. IV. 1960 presented)

## První sdělení.

Příznivé zachování fosilních zbytků obratlovců, především savců *(Mammalia)*, které by umožňovalo podrobné mikroskopické vyšetření jejich histologické stavby, náleží v historii paleontologického výzkumu našich zemí k největším vzácnostem. Proto bylo do jisté míry nečekaným překvapením, když v několika blíže systematicky neurčitelných fosilisovaných zbytcích měkkých tělesných částí pleistocenních savců (kosterní svalstvo, periartikulární vazivo, úpony šlach na kosti, část páteře s míchou a dva savčí mozky velkých druhů) se podařilo bezpečně zjistit zachované histologické struktury. Jejich podrobnému paleohistologickému vyšetření je věnována tato práce.

Autor považuje za svou milou povinnost poděkovati zde svému dlouholetému příteli Jaroslavu Petrbokovi za poskytnutí tohoto nejvýše zajímavého studijního materiálu.

Níže popisované paleohistologické objekty pocházejí vesměs ze známého naleziště v pleistocenních travertinech riss-würmského stáří, odkrytých v lomu „Hrádok" u obce Gánovce blíže Popradu v Liptovské kotlině na Slovensku.

Bohaté osteologické, malakozoické a paleobotanické nálezy, zde učiněné, byly již dříve zhodnoceny (Franzé R., Kiss P., T. Kormós, M. Staub, A. Scherffel, F. Pax).

Materiál zde popisovaný byl zachráněn sběry J. Petrboka v létech 1923—1925.

Teplomilná malakofauna (*Helicogena pomatia L., Fruticola strigella* Draparnaud, *Tachea vindobonensis* Férussac, *Eulota fruticum* Müller, *Carychium speciosum, Limnaeus palustris* Müller), kterou získal Petr-

bok z různých vrstev po odlomu tvrdých travertinů, mu byla určovacím znakem riss-würmského interglaciálu.

Další nálezy mozku *(Rhinoceros)*, karapax *Emys orbicularis* L., odlitek nosní přepážky a petrifikované konchy *(Equus* sp.), ztracený úlomek dolní čelisti se čtyřmi stoličkami *(Rhinoceros)*, dva mnou vyšetřované mozky neznámých savců a mozek *Hominis neanderthalensis* patří mezi tyto vzácné objekty.

Flora těchto travertinových vrstev je charakterisovaná výskytem druhů: *Picea excelsa* L., *Pinus silvestris* L., *Corylus avellana* L., *Betula* spec., *Quercus pedunculata* L., *Carpinus betulus* L., *Salix caprea* L., *Salix cinerea* L., kterou zpracoval F. Němejc.

Roku 1953 popsali v kolektivní studii M. D. Eman. Vlček mozek *Hominis neanderthalensis* i s ostatním osteologickým Petrbokovým materiálem ve Slovenské archeologii (Akádemia vied, Bratislava).

Uvedené práce se zabývaly stratigrafickým a makroskopickým zhodnocením nálezů. Nikdo se nepokusil o mikroskopický výzkum v předpokladu, že tvrdý travertin není vhodný pro histologická vyšetření.

Po zevrubném zjištění studovaných materiálů jsem si rozdělil mikroskopické zpracování z hlediště embryogenetického na deriváty:

I. prvního zárodečného listu (neuroektoderm) — mozkomíšní tkáň s nahodilým nálezem petrifikovaných chlupů),

II. a třetího zárodečného listu (mesoderm), kostní typy, kosterní svaly, šlachy, hlenotvorné váčky (bursae mucosae), systém arteriovenosní, systém lymfatický, systém retikuloendotheliální krevní — systém retikuloendotheliální lymfatický, zárodečné buňky řady erythropoetické (haemoglobinogenní), zárodečné řady buněk lymfatických (enzymogenní).
Systém petrifikované krevní plasmy a haemolymfy. Přeměnu haemolymfy v lymfu se zvláštní světelnou vlastností při šikmém osvětlení mikropreparátů seshora.

Nové mikroobjekty jsou: filtrační zařízení haemolymfy s filtračními štětcovitými štěrbinami, filtrace a koncentrace haemolymfy a lymfy v lymfatických váčcích. Rozdělení filtrátu v kapilárách přes makroendothelie vsunutých lymfatických kapilár s výraznou infiltrací jejich cytoplasmy, která v šikmém osvětlení v buňkách svítí. Argentaffinní systémy retikuloendotheliální haemoglobinogenní a argentaffinní systémy retikuloendotheliální lymfogenní.

Nativní mikroobjekty dávaly nejlepší pozorovací výsledky. Dobarvování histochemickými barvivy (eosin, methyl. modř Giemsa, čínská tuš a impregnace dusič. stříbrnatým) dalo dobré zkušenosti. U různých mikroobjektů jsem používal projasňovacích medií podle povahy preparátů zcela různých, abych jimi neporušil jejich přirozenou brilanci (ol. cedri, ol. Origani, ol. terebinthinae) a přes xylen jsem montoval do různě hustého kanadského balsámu.

Tkáňové systémy (cévy) i jednotlivé buněčné útvary (krvinky) se proměnily ve sklovitě křehké průsvitné útvary s třírozměrnou plasticitou a mikroreliéfovou tvárností kostních buněk, (řasinek), neuritů a dendritů.

Přirozená barva těchto mikroskopických, petrifikovaných útvarů vznikla z biogenetických prvků, kterými byla živá hmota prosycena (C, Fe, P, Mn, Mg, S a vedle stopových prvků to byly i hojné plyny).

Podle převládající barvy je možno rozeznávati dvě základní vedoucí barevné složky. Žlutá a její odstíny patří krevnímu systému obsahujícímu Fe dýchací pigment, vázaný na všechny fysikálně chemicky změněné deriváty haemoglobinu. Barva voskově šedá, světlo pohlcující se všemi odstíny čínské tuše, ozokeritu až asfaltu je vedoucí barvou různých derivátů fosforu v buňkách i jádrech (řady enzymogenní) lymfopoetického systému, včetně lymfy a epiteloidních buněk vzhledu lipofagů. Další kombinační odstíny obou barev v podobě rezavých, nebo hrudkovitých plochých špinavě šedožlutých hromádek (haemosiderin) i rozplihlých skvrn nalézám na povrchu kostí, které byly vystaveny působení povětrnostních změn a podle jejich mikrostruktury jde o druhotné anorganické metamorfosy Fe a P.

Barvu tuhové šedi mají všechny buněčné útvary centrálního nervstva (glia a gangliové elementy).

Tabul. No. V. fig. 1 (a.) I. zobrazuje zlomený fosilisovaný chlup. Základní hmota je světlolomná a světelnou interferencí vznikly střídavě tmavé a světlé pruhy. Zlom obnažil dřeň s čárkovitými buňkami i zbytky jejich jader. Fig. 1. Jádra korových buněk prominují, jsou vejčitá, smolově černá. Na mnohých místech zvlněného chlupu je dvojlom světla.

Fig. 1 (b.) I. zobrazuje objemnější chlup opět rozdělený na čtyři podélně světlolomivé pásy. Na hrotovém zlomu je utvořena podkovovitá kresba určující dlouze vinuté zakřivení chlupu.

Fig. 1. (c.) I. zobrazuje chlup stejně objemný předešlého s nalomenou částí míšku (follicul). Vlastnosti buněk a jader dřeně i kory jsou shodné jako u předešlých exemplářů.

Všechny tři chlupy jsou prostoupeny kalcitem. V šikmém zástinu jádra buněk kory prominují a všechna jádra mají vlastní i vržený stín.

Mozková tkáň (šedá a bílá hmota) je proměněna na mikroskopické drůzy kalcitu, apatitu, chlorapatitu a fluorapatitu, které obsahují inkluse nervových buněk (gangliových-gliových), podpůrnou tkáň s různými výběžky (dendrity, neurity a jemnou jejich plstí).

Tabul. No. VI. fig. 2 (a.) I. 1+2. Fig. č. 2 zobrazuje polyedrické gangliové buňky s ulomenými neurity o dendrity (velikosti asi 10 $\mu$).

Fig. 2. (b.) I. 3. zobrazuje trojúhelníkovité gangl. b. s perinukleárním jasným dvorečkem (vel. 15—20 $\mu$).

Fig. 2 (b.) I. 4—5. gangliové buňky s tygroidní hmotou v cytoplasmě (15—20 $\mu$), fig. 2. (c.) I. 6, 7, 8, 9. velké gangl. b. přes 30 $\mu$, mnohé se dvěma jádry.

Prosycením mozkové hmoty kalcitem a jeho rekrystalisací vznikly planparalelní dvojlomné mikroskopické destičky (tabul. No. VII. fig. 3. (d.) I glia 5 — v míše — obj. No. III. makroobj. Tabul. XXXIV. — mnohdy tak silné, že vznikl rastr s mnohými inklusemi všech ganglio-gliálních kostrovitých stínů se světelnými ohybovými interferencemi.

Stereotypní uspořádání stínů buněčných těl i jejich výběžků dává záruku, že ve stejných nálezech z různých míst jde o pozůstatky bývalých

neurogliálních a ganglionárních buněčných struktur. Tabul. No. VII. fig. 3. (d.) I. glia 1., 2., 3., 4., 6., 7. Normální histologické rosetovité uspořádání glie tento názor potvrzuje fig. 3. (d.) I. glia 8., jakož i zbytky kapilár v gliální síti uchovaných fig. 3. (d.) I. glia 3.

Holá osová vlákna i s pochvou a obrazci Ranviérovými Tabul. VIII. fig. 4. (e.) I. 1. a fig. 4. (e.) I. 2. je vzácný nález. Také zdvojené neurity fig. 4. (e.) I. 3. I. 4. I. 6. 7. a zachované dendrity fig. 4. (e.) I. 5—I. 6. jsou těžko k nalezení, ale svým bizarním vzhledem se prozradí. Impregnace dusičnanem stříbrnatým dává mikrostruktury podobné těm, které získáváme metodou sec. Golgi. Tabul. No. IX. fig. A. (a.) 1. // II. oss. (a.) 2., (a.) 3. — zobrazuje Haverské systémy deskovitých kostních vějířů z plochy, šroubovité uspořádání desek s kapilárou vyživovacího Haverského systému, včetně šikmých kapilárních anastomos mezi paralelně položenými Volkmannovými kapilárami. Fig. A. (a.) 4. // II. B. art. ven.

Novotvořené kapiláry ze dvou až pěti endothelií (Tabul. X., fig. A. (a.) 6., (a.) 8., mají na basi buněk stěny zoubkovitý lem, jak je patrný na isolovaných endotheliích fig. A. (a.) 9. // II. Tab. XI., fig. B. (b.) 1. // II., tabul. No. XV. fig. B. (c.) 4. // II. a retikuloendotheliích Tabul. No. XV. fig. B. (c.) 1. // II., fig. B. (c.) 2. // II., fig. B. (c.) 3. // II., fig. B. (c.) 5. // II., fig. B. (c.) 7. // II., fig. B. (c.) 8. // II.

Kapiláry arteriovenosního systému jsou jednak uvnitř kostí a jednak na přechodech svalů do šlach a okostice. V kostech jsou to systémy Haversových a Volkmannových vyživovacích arteriol, které po prostoupení skrze kostní otvory šikmo prostupují do kostní dřeně, aniž by do ní volně vyúsťovaly. Druhý typ jsou šroubovitě vinuté arter. helicinae vytvořené v místech tlakem a tahem svalů vysoce namáhaných. Tvoří přeslenovité větve hadovitě vinuté, které mají schopnost dobře se rozvinout do délky, aniž by při zvýšeném krevním tlaku praskaly. Mnohé jsou opatřeny svěračem a mohou postranním oběhem převádět krev do krevních zásobních rezervoárů, tabul. No. XI. B. (b.) 3. XII. B. (b.) 6, XIII. B. (b.) 10, figura č. 3, tabul. XIV, fig. B. (b.) 17 // II., B. (b.) 19. Fig. č. 3.

Kosti houbovité tvoří trámčinu v konečných částech a v hlavicích dlouhých kostí rourovitých. Mají větevnatou strukturu a mezi těmito jemnými trámečky jsou husté systémy krevních splavů většinou naplněných vývojovými stadii červených krvinek / Tabul. XVIII. fig. B. (c.) 15. II., (c.) 16., (c.) 17,. (c.) 18., tabul. XIX., B. (c.) 20. II., (c.) 19., (c.) 22.

V těchto houbovitých kostech je nejhustší vyživovací krevní síť Haversových kapilár.

Kapiláry tvoří úzké kanálky naplněné okysličenými krvinkami oranžově červenými, kteréžto petrifikované miniaturní krevní válečky nasedají na svazky světlolomných, sklovitě jasných štěrbin. Štěrbiny tvoří štětce, jimiž souvisí arteriální systémy se štětcovitými štěrbinami sklovitě průsvitnými sousedních lymfatických kapilár. Tímto způsobem vznikají nevídané útvary na koncích obou systémů (krevního a lymfatického) jakési primitivní štěrbinové filtry mající rozměry cca (80 $\mu$ × 90 $\mu$ × 120 $\mu$). Tímto způsobem je vytvořena interkalární filtrační zóna, která přechází asi 70 $\mu$ dlouhou kapilárou do lymfatického cirkulačního systému (tabul. XXI, fig. B. (d.) 12., 13., 14.), který je sklovitě lesklý bez-

buněčný s čárkovitými temnými stíny v místech, kde normálně bývá endotheliální výstelka.

Po zaclonění kondensoru v šikmém osvětlení tato 10 $\mu$ silná kapilára růžově svítí až po velkou kupovitou buňku (makroendothelii), která celou svítící část kapiláry uzavírá. (Tabul. XVII. fig. B (c.) 9., (c.) 10., (c.) 12., tabul. XX. fig. B. (d.) 1. tabul. XXI, fig. B. (d.) 6., tabul. XXV., B. (d.) 26., 27. ku poctě nálezce gánoveckých unikátů ji nazývám „buňka Petrbokova".

Mimo štěrbinovité filtry, právě popsané, nacházím další filtrační lymfatické vakovité útvary, do kterých se arterioly zanořují a v nich se větví. Pravděpodobně osmosou v nich vzniká haemolymfa růžově prosvítající v šikmém zástinu. Na periferii váčků, kde se v kontaktu s dvojvrstevnou výstelkou váčku mění haemolymfa na bíle svítící lymfu, nastává intensívnější bílé svícení hmot, které v procházejícím světle byly kouřově šedé a voskově matné. (Tabul. XX. fig. (d.) 3., (d.) 4., (d.) 5., tabul. XXII. B. (d.) 15., a.—b., tab. XXIV. B (d.) 20., 21., 22., až 25., tabul. XXV. (d.) 26. až 29., tab. XXVI. B. (d.) 30. až 35., tabul. XXVII. B. (d.) 36., 37., 38., 39., 40., 42. Tmavé hmoty světlo pohlcují.

Filtrační lymfatické vaky mají v interkalárních kapilárách velkou makroendothelii Petrbokovu, která v řadě srovnání a studií na materiále z makroobjektu IV. (Tab. XXXIV.) kost č. 1—2—3 dávají možnost výkladu o její uzávěrové funkci (pressorické) na místě uzávěrové chlopně.

Retikuloendothelie zárodečných zón v houbovitých kostech mají argentaffinnitu. Jedna řada těchto buněk má cytoplasmu i jádro zbarveno žlutě až do oranžova a může se funkcionálně adaptovat na vývojovou řadu červených krvinek se všemi barevnými znaky haemoglobinogenních útvarů (erythroblasty, erythrocyty, ovalocyty, mikrocyty, arteriovenosní endothelie). Druhá řada se funkcionálně adaptovala na osteogenní funkci se všemi barevnými znaky žlutého Fe dýchacího pigmentu. Veliké retikuloendothelie se hrubými zoubkovitými kartáčky zanořují do kostní hmoty směrem k první řadě osteocytů, s nimiž jsou zoubkovitě pilovitým lemem v kontaktu. V cytoplasmě se hromadí hrudkovitý žlutý Fe. pigment, buňky se mění v dlouze vřetenovité, obdávají se kostní hmotou a zanořují se do hloubky tvoříce útvary podobné osteoblastům. Mají zachovanou argentaffinnitu původních neutrálních retikuloendothelií. / tabul. XV. fig. B. (c.) 1. / I., (c.) 2., (c.) 3., (c.) 5., (c.) 7., (c.) 8., tabul. XVI. B. (c.) 4. —. — tabul. XVII. fig. (c.) 7. / II. (c.) 8.

Argentaffinní retikuloendothelie tvoří jemnou síťovitou plst mezi endotheliální výstelkou arteriovenosní i endotheliální výstelkou lymfatických cév. Vznikají zde husté oxydoredukční argentaffinní mřížky (tab. XVIII. fig. B. (c.) 14. / II. dýchacího systému Fe i enzymogenního systému fosfokatalysačního. ($O\text{-}CO_2\text{-}N\text{-}H$.)

Šedé retikuloendothelie v dřeni cylindrických dlouhých kostí jsou voskově matné a pohlcují procházející světlo. Jsou argentaffinní a na basi mají zoubkovitě kartáčkovitý lem. V dopadajícím světle jejich cytoplasma bíle svítí, zvláště u typu makroendothelií Petrbokových, Tabul. XXI., fig. B. (d.) 6. / II., (d.) 8., tabul. XXIII. B. (d.) 18., (d.) 19., tabul. XIX. fig. B. (c.) 23., (c.) 24., tabul. XXV. fig. B. (d.) 26., 27., 28., 29., tabul. XXVI. B. (d.) 34., (d.) 35., tabul. XXVII. fig. B. (d.) 38., 39., 40., (d.) 42.

Ve dřeni rourovitých kostí jsou lymfoepitheloidní veliké buňky s malými jádry vzhledu lipofágů a po jejich vyzrání se v cytoplasmě hromadí šedé granulace makro-granulocytů, velkých bloudivých, bílých krvinek. Tabul. XIX. fig. B. (c.) 21. / II., (c.) 25., tabul. XXI. B. (d.) 10 / II.

V houbovitých kostech vznikají převahou červené krvinky, které po vypuzení jader jsou schopny další funkce v cirkulující krvi jako útvary bezjaderné. V dutých kostech rourovitých se tvoří převahou krvinky bílé makrogranulocyty, které nacházím převahou jenom v kostních cévách lymfatických a v jejich filtračních systémech.

Na rozhraní dvou chemicky různých prostředí jsou vytvořeny argentaffinní oxydoredukční mřížky, které pravděpodobně regulovaly oxydaci v pericelulárních argentaffinních štěrbiách kostních buněk, jež si zachovaly ve všech stadiích vývoje původní argentaffinnitu zárodečných retikuloendothelií.

Po objektivně zjištěném funkcionálně diferentním dvojím různě barevném systému Fe a P je přijatelný výklad o dvou antagonistických systémech:

1. oxydoredukčním systému Fe haemoglobinogenně adaptovaných retikuloendothelií, který obstarává základní biogenetické reakce dýchacího pigmentu a
2. oxydoredukčním systému fosfoenzymogenním, který obstarává základní reakce katalysační za přítomnosti hmoty, která v petrifikované lymfě v šikmém zástinu svítí bíle a v petrifikované haemolymfě svítí růžově.

Kostní tkáň tentorii cerebelli jsou zkostnatělé mozkové blány (dura mater), které svojí mikroskopickou skladbou jsou shodné s uvedenými znaky již popsaných kostí plochých. Diploe, houbovitá střední vrstva je silně cévnatá. Totéž platí o struktuře plochých kostí z clivus Blumenbachii.

Ve stěnách mozkových cév je melanoidní pigment.

Důležitou složkou třetího zárodečného listu (mesodermu) jsou vazivové buňky, které jsem nalezl v plsti utvořené ve stěnách velkých cév krevních pomíchané se šlachami a kosterním svalstvem. Tvoří hustou mřížku příčně i šikmo uspořádaných vláken špinavě žlutavých. Tabul. XXVIII. fig. C. (a.) 1. / II., fig. C. (a.) 2. / ., (a.) 4.,

Myxofibromatosní vazivo tvoří hlavní složku periartikulárních měkkých částí a k nim patří i hlenotvorné váčky (bursae mucosae). Rozlomeny upomínají na lískové oříšky a jsou systematicky uspořádány v prostoru mezi kostmi a přilehlými měkkými částmi kosterního svalstva. Je jich volně studiu přístupno šest a mají rozměry: 10×14 mm, 9×6 mm, 18×6 mm, 16×10 mm, 20×10 mm, 10×6 mm a tloušťka stěn je 2 mm.

Stěny sestávají zhruba ze tří nosných brilantně třpytivých jemných krystalů, které v osách krystalisačních mřížek obsahují zbytky buněk a jader, myxofibromatosních křídlovitých buněk, zvláště dobře patrných ve dvojlomném kalcitu (Fig. č. 4) a Tabul. XXIX. a XXX. C. (a.) 5., až C. (a.) 15 / II.

Kosterní svaly tvoří na makroobjektu IV. (tab. XXXIV) přesně odlišitelné celky. Zhotovením mikroreliéfů a rozdělením jednotlivých políček jsem získal přehled o důležitých zónách a po dlouhém hledání jsem našel přesvědčivé modely konvexkonkávních mikroreliéfů, Tabul. XXVIII. fig. C. (a.) 4. // II. a isolované příčně pruhované vlákno se zbytky interstitiálních vazivových buněk na obvodě. C. (a.) 3. / II.

## Závěr

Paleohistologické vyšetření čtyř makroobjektů (mozek tab. XXXI až XXXII., petrifikované obratle s míchou (tab. XXXIII.) a petrifikované kosterní svaly se šlachovými úpony na kosti (tab. XXXIV.) dalo řadu nečekaných histologických výsledků. Petrifikované buňky a celé tkáňové systémy jsou dobře zachovány a mnohdy i v detailech dobře rozpoznatelné. Buňky jsou jemné útvary neobvyklé krásy, mnohdy sklovitě průsvitné v přirozených barvách, takže jejich vzhled je originální.

Argentaffinnita jednotlivých tkání a buněk, jakož i dobarvitelnost jejich histochemickými barvivy byla zachována.

Nejpozoruhodnější vlastnost bývalých organických hmot je jejich svit v dopadajícím šikmém světle. Lze jej vystopovat ve funkcionálně specialisovaných úsecích lymfatických a haemolymfatických cirkulačních systémech, a to od kapilár až po filtrační váčky.

Je přijatelný výklad o biogenetické povaze tohoto svitu, který mohou vydávat funkcionálně adaptované, biogenetické, stopové prvky.

Výzkum tohoto pozoruhodného efektu bude sdělen ve druhé části obecného pojednání.

# Paleohistological researches in Riss-Würm travertines in the area Hrádok-Gánovce near Poprad

## First communication

There have been fossil researches with osteologic and phytopaleontologic materials in Gánovce-travertines since 1881 (P. Kiss, M. Staub, A. Scherffel, R. Franzé, T. Kormos, F. Pax).

This region was investigated in 1923—1925 by Petrbok Jaroslav, scientific associate of the National Museum in Prague. He gathered an outstanding material which had not been still found in Gánovce by anybody.

Malacophauna of the interglacieral period (*Helicogena pomatia* L., *Fruticola strigella* Draparnaud, *Tachea vindobonensis* Férussac, *Eulota fruticum* Müller, *Carychium speciosum, Limnaeus palustris* Müller in various travertine-layers offered him a precious determining material of the riss-würm period).

By further chipping off the hard travertine material he gained petrified brains (*Rhinoceros* one, two indeterminates) and petrified brain belonging to the *Homo neanderthalensis* group.

A unique finding (recherche) has been a set of skeleton muscles, tissue, bones and bursae mucosae. Further casts contain the nose septum and nasal conchae (*Equus* sp.), karapax (*Emys orbicularis* L.), vertebras from the column.

A rarely well preserved phytopaleontological material was fixed and worked up by d. F. Němejc.

E. Vlček, M. D. completed the osseous material in collective study from the Slowak Archeology 1953 (Academy of Sciences in Bratislava).

The mentioned works were chiefly interested in stratigraphy and macroscopical diagnosis, but nobody tried a microscopical evaluation because the material had been supposed as unfit for.

In fall of 1959 I made several microscopical slides which created some unawaited material.

I.) Ectodermal derivates (petrified hair, brains and spinal marrow).

II.) Mesodermal derivates (various types of osseous architectonics, systems of blood and lymphatic circulation, evolution types of red and white blood corpuscules, reticuloendothelial lymphatic and blood cells, striped muscles, myxofibromatous and reticular structures, argentaffine system).

An improtant finding is that of haemolympha opalescency in a petrified homogenous tissue of lymphopoetical systems and that of filtration arrangements in arteriovenous capillaries at the place of transition in lymph capillaries.

Main slides gave best results. Staining of microobjects with methylene blue, eosine, Giemsa-Romanovský, van Gieson, China-ink, and argent nitrate and using the polarisating microscope was succesful and we gained much wellcomed experiences.

As clearing medias we used Ol. cedri, Ol. terebinthinae, Ol. origani and via xylol prepared for the Canadian balsam.

The tissue systems and even single cells had been well preserved by the changes of biological structures and changed in tender glasslike microobjects with all space plasticity of their microreliefs and galvanoplastical reliefs (bonne, cells, oligodendroglia).

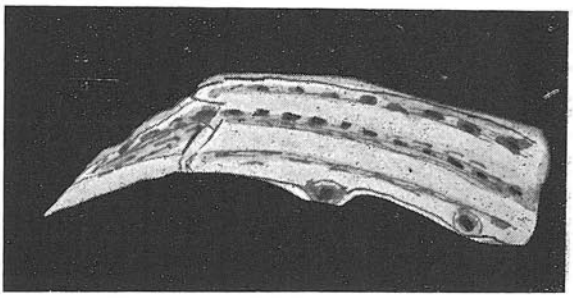

Fig. 1. Schodovitě ulomený fosilisovaný chlup s obnaženou dřeňovou vrstvou.
The fossilicated staire-case-like broken off part of the hair. The hair has a glassy transparency and marrow cells differ remarkably.

The native colour of salt derivates (Fe, Co, S, P) and the luminiscency of petrified tissues has an original lock.

Various lines of yellow and gray belong into the category of carbon metamorphoses in space and time. Valencies of C, P, Ca, Cl, As, S, Co, Mg, F, Fe, in immense pressures and temperatures melted the biological structures with aid of O, H (He?-N), into fine nuances of China-ink, graphite, ozokerit and asfalt.

Fine cytoplasmatical structures have been preserved by nearly all cells of the ectodermal part.

Tabul. No. V. / Fig. 1. (a.) I. contains a sickle-shaped hair, which is narrowing toward the end. Both ends of the hair are broken off. After breaking off the fossiled point there emerged a staircase-like picture. The lower part of the hair is wedgeshaped and contains a cortical layer of cells with nuclei. A farther part of the breaking interferes (touches) with the marrow. This marrow has a glassy transparency, cylindrically shaped, its cells are elliptics with distinct pitch black nuclei and form a continuous line from the point to the broken off end. Fig. No. 1. Cortical and marrow cells differ (reflect) remarkably from the homogenous glassy mass of the hair.

In oblique (side light) micro-technique we find along the whole length of the hair two dark and two light-breaking stripes. Nuclei of cortical and marrow cells are pitch black.

Fig. 1. (b.) I. Is broader then the above mentioned hair. Once more the ends are broken off, the whole length represents a glassy transparency, being divided in two longitudinal dark stripes and two light-breaking stripes, the one following in term the other. Nuclei of the hair cortical cells are pitch black, round, prominent. The marrow-cell nuclei are elliptic in similarly shaped low flat cells and are pitch black.

Fig. 1. (c.) I. contains a third hair with a broken-off end and with a broken off part of follicle, shaped bulb-likely. Nuclei of cortical cells are elliptical with smaller elliptical nuclei. The nuclei of both layers are not transparent and pitch black. The mass of this petrified hair is light-breaking and again divided in two dark and two light stripes, which can be seen throughout the whole hair. On the hair fracture we can easily distinguish each of these stripes in the form of light breaking circles, which reminds us of horse-shoes, by this horse-shoe profile being determined the curvature of this hair as well.

All three hairs are full of the main light-breaking substance ($CaCo_3$). Marrow and cortical cells form 4 longitudinal stripes. The nuclei of cortical and marrow cells are opaque, pitch black. In oblique micro-technique cortical nuclei are projecting, have their own shadow and cast a shadow. The bristles are of yellow gray colour.

Cerebral tissue of the first macroobject (Tab. XXXI.) is full of mineral masses, found in microslides as bunches of microcrystals. Neural cells of the gray matter and white matter axons as well had been impregnated and filled up with previously mentioned salts. Their basic biologic structure was changed in various carbon derivates by overcrystalisation of carbon structures with the aid of high pressures, being pressed and pulverised.

I have been able to examine cellulous petrified masses in parts of cerebral tissue there, where white corrosions had been formed and those places, which had been covered by rests of original head skeleton.

I could roughly divide the gained cell-microobjects in three parts. Mostly we find cells grown into crystals or pressed (printed) on micro-crystals.

Tabul. No. VI. Fig. 2. (a.) I. 1. Small, round erythrocyte-sized cells (7—10 $\mu$) stretched into tips, without neurites or dendrites. Cytoplasma abundant, nuclei vesicle-like, among fine granulated grey substance reminding us of tygroid. Plasma is dull gray, the nucleus orage. Fig. No. 2.

Fig. 2. (a) I. 2. Big triangular cells with lemon yellow cytoplasma and clearer perinuclear area. The nucleus is large, vesicle-like, pitch black and sometimes placed outside the center.

In some these cells there are two red and orange nuclei with two pitch black nucleoli each. The cytoplasma of both these types has a fine gray granulation (tygroid substance).

Fig. (b) I. 3. Large over 30 $\mu$ big tipped cells, nuclei vesicle-like and rusty brown, the tygroid substance yellow, light breaking. Appearance of the cells is waxy dull.

These three mentioned kinds of different cells I have found in tractus olfactor. cerebri No. I. (Tab. XXXI.), in gyr. parietooccipital. and in regione pontis cerebri (Varoli) No. II. (Tab. XXXII.)

Neural matter gained from a fossiled vertebral column (macroobject. No. III.) (Tab. XXXIII.) showed us a sandy yellowish stuff, similar to the corroded white matter of both brains. From this stuff I prepared a number of native and silver impregnated slides with three kinds of ganglion cells.

Fig. 2. (a.) I. 1. Small round ones sometimes tipped with an orange nucleus and a lemon like yellow tygroid substance, finely dispersed in the perinuclear area. The cell nuclei are round, sometimes excentrically placed, pitch black.

Fig. 2. (a.) I. 2. Large polyedric cells over 20 $\mu$, sometimes like long triangles with lemon yellow plasma and gray granulated perinuclear

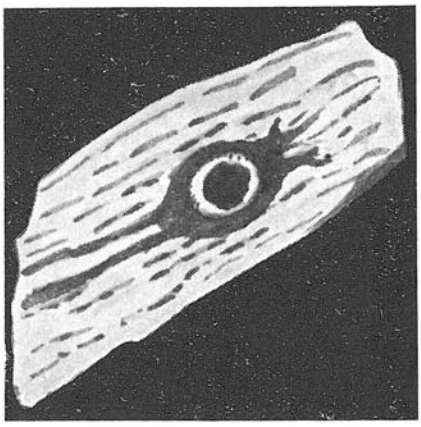

Fig. 2. Gangliová buňka s ulomenými dendrity a se dvěma neurity.
Ganglionaire cell with some dendrits broken off doubled neurits.

tygroid substance. Large pitch black and bullous nuclei. In some ganglionic microobjects orange-yellow nuclei may be found. These cells have a dull waxy appearance.

Fig. 2. (b) I. 3. Large polyedric over 30 $\mu$ big cells with mainly dendrites broken and doubled neurites (microfoto: Tabl. VIII., fig. 3. (e.), 4. (e.), 7. (e.).

Tabul. No. VII. Fig. 3. (d.) I. Glia. An important finding are neuroglial mesh-like substances, tabul. No. VII., fig. 3. (d.) I glia 1., (d.) 2., (d.), 3., (d.) 4., (d.) 6., (d.) 7., (d.) 8. with fragments of cerebral and columnar capillaries with meshwork full of ganglion cells.

Oligodendroglia is more, large astrocytes form pitoresques ramificated meshworks coloured graphite gray and strongly argentaffin (microfoto: tabul. VII. fig. 3. / 1. (d.).

Naked axons are rather rare we can follow them only, briefly after emerging from the cells. Pieces of neuroaxons and further isolated axons may be found when carefully studied.

Naked neuraxons are light breaking and in side light microtechniques show a distinct myelin sheath with incisures (Ranvier) and with dark networks on narrowed places (microfoto: Tabul. No. VIII. fig. 1. (e.), fig. 2. (e.).

The native colour of myelin (sphingomyelin) and neuroaxons is a slate-gray or graphite black dull and preserves argentaffinity. Several neuraxons form bundles of various flat breaks, graphit-bright with transvers incisures.

II. Mesodermal derivates.

A.) Osseal tissue of:
  a.) flat, cover bones of the scull
  b.) structures of spongious bones
  c.) the compact mass of long bones
  d.) the ossified tentorium cerebelli
  e.) clivus Blumenbachii

B.) Blood vessels (a, b, c) B. (d. Haemolymphatic and lymphatic systems).

C.) Fibrocytes, leiomyocytes, skeleton muscles, tendons and bursae mucosae.

II. A) a. The flat metamorphosed bone tissue forms fans of Haverse channels. The layers are sometimes diversed from one of the three principle dimensional axes (x, y, z) according to the pressure effects (static and dynamic), which modelled the graduated layers of plat bones. The layers are sometimes torsioned and we find screw-like systems with smaller or broader threads. We find the bone-cells radially lined in these layers. Dendritic structures, outstandingly accepting silver compounds are sometimes to be found in cavities with bone-cells. And by forming these layers we can find innumerous networks, brightly shining and darkening in polarisation microscopes.

Vessels which we are able to differ in blood and lymphatic systems, have been pressed in among the flat bone layers.

II. B. (a.). Blood capillaries of the arteriovenous system are fairly wide for cells of the erythrocyt, macrophage or blood platellets group. Their walls are produced by a single reticulo-endothelial cell layer (15 $\mu$), the outer basal part of which is covered by a brushy lining. These brushes are minute and turned towards the blood-flow. These teeth-like brushes correspond perfectly with dimples in the surrounding bone, performing a fine argentaffine meshwork. Naked vessels can be found and studied from both sides when emerging from many specimens after the break-off bone-layers. In (oblique) side light microscopy techniques we gain a picture of micro contours. Basal parts of endothelial cells with large ball-like nuclei are easily distinguished on the surface of out peeping capillaries. Petrified and homogenous plasma is orange the endothelial nucleus colour is siena-brown. Brushy edges on broken-off and isolated single endothelials are easily distinguishable. (Tabul. No. XI., fig. B. (b.) 1.

Blood vessels are mostly divided in various directions. That is how little, plastically modelled channels with mosaic walls originated.

Inside some vessels we can see at the point of breaking the beginning of capillaries with many white and red blood corpuscles.

Endothelial and red blood cell plasma is golden and yellow, all cell nuclei are amber brown. Basal parts of endothelial cells are brushy, forming minute combs of yellow colour. Various hues of capillary colours can be demonstrated on vessels filled with erythrocytes, which are pressed in yellow petrified blood plasma.

Amorfous plasma forms yellowish thrombus-like cylinders, with amber brown erythrocytes. In vessels of higher grade (II and III) are even big white macrophage-granulocyte cells (Tab. XIX.) [fig. B (c.) 25].

Homogenized clots of blood plasma are full of fibres arranged in fibrin reticulas. These networks with white and red blood corpuscules as well fill long parts of bigger vessels. These described structures bear

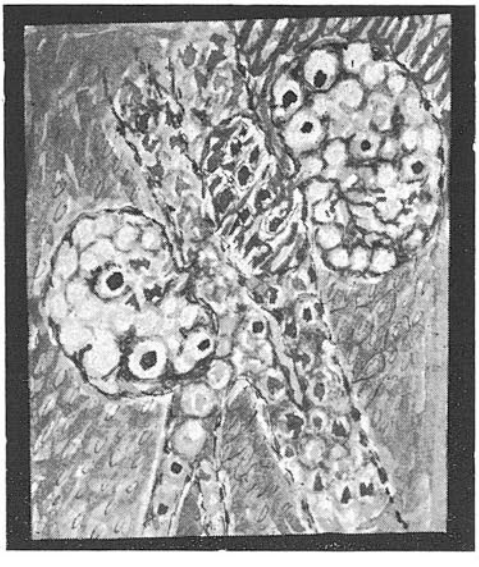

Fig. 3. Krevní vaky na helicinních arteriolách.
Microscopical blood sacs (aneurysma) on the wall of arter. helicines.

many similarities with normal blood-clotting but are not being found in all higher grade vessels. Mostly in places of tendon and muscle insertion on bonnes. Vessels have a characteristic appearance there.

Larger second and III$^0$ (third) grade arteries with all their wall-layers (intima, media, adventitia) divide in special places. In one place emerge 3—5 collaterals, turning against the main current of the mother artery in tortuous and spiral capillaries and resembling us of helicinae arteries.

In case of an unexpected blood-pressure rising they straighten and thus help to overcome the stress on blood circulation.

On diagonal break points of larger vessels we find several layers of a muscle network with elastic fibres and tissue cells, all of these cells being eliptic and longitudinal with sharp endings. Cytoplasma is yellow and the nuclei are amber-brown. Above the beginning point of collaterals is the wall of the mother vessel strengthened by 5—7 layers of circular cell rings, forming a sphincter. [Tabul. XII., fig. B. (b.) 5, (b.) 7, (b.) 9.]

After the beginning of helicine collaterals the wall of each mother vessel is reduced into a sort of aneurysma (cavity) of 2—3 layers, covered with endothel. Fig. No. 3.

This microscopical aneurysma is longitudinally eliptical above the bone surface. Arteries, ectatic blood sinuses with endothelial insides

occasionally immerging in bones begin, where these sac-like dilatations end.

All of the vessel structures described here are in native microobjects plastic and have glassy bright elliptic surfaces with dark spots, where the sac walls are lowered. These vessel structures functioned as relieve reservoirs, similar to rete mirabilis found by whales. Sacs are filled with all sorts of blood-elements, the way it can be found on some broken specimens. [Tabul. XII., fig. B. (b.) 6, (b.) 8.]

Lymph vessels are one-layered tubes of various diameters, usually somewhat broader than blood vessels. A single endothelial layer of large epitheloid cells forms their inside. The cells are polyedric with undulated edges, the waves being in close contact with cavities of neighbouring cells, thus constructing a tapetum inside lymf vessels, sinuses and sacs. [Tabul. No. XX., fig. B. (d.) 1., (d.) 2., (d.) 3., (d.) 4., (d.) 5.]

When studying the endothelial cells on a diagonal breaking point of the vessel walls, we are able to find ciliar trimming of cells bases, sitting closely in bone lacunae and forming structures similar to chorionepitheliomatous specimens, known from histopathology. In oblique micro-techniques the ciliar trimming in rather light-breaking and thus an optically free patch originates between the endothelials and bone mass. [Tabul. No. XV., fig. B. (c.) 1., (c.) 2., (c.) 3., (c.) 4., (c.) 5., (c.) 6., (c.) 7., (c.) 8.]

Homogenised and petrified lymph mass in native microspecimens gray, resembling ozokerit.

Lymphoepitheloid cell nuclei are large and bulous, pitch black. Cylinders of mineralized dividing lymph vessels are pressed in among flat bone lammelae. After breaking off the top or lowest layer we are able to study the gray, cylindric, homogenized lymph masses with pressed in epitheloid cells. Large, finely granulated macrophage cells with grey plasma and a pitch black nucleus (sometimes excentrical) stick inside these grey cylinders in groups of five or more.

In obliques micro-technique and whenever a veil is used the gray homogenised lymph masses appear rosy. Macrophage cells luminate like glass-pearls.

This has been a brief description and photomaterial of vessel pecularities of flat bones, belonging to the macro object No. IV. Further peculier arterivenous structures have been described and a queer luminosity of lymph capillaries and vessels.

II. A. (b.) Spongious bones form chiefly Haverse system, arborized, from a mineral bone mass. The bone structure strengthens and overarches epiphyses and diaphyses of long tube-like bones. According to the organism's static and dynamic dispositions simple or compound Haverse-systems grow into each other, performing a dichotomical ramification and anastomosing with blood ad lymph sinuses. On longitudinal fractures of Havers systems multiple blood capillaries (Havers, Volkmann) can be found. They penetrate the outer part of the bone, run obliquely through the compact mass and are buried in bone marrow (arter. nutritivae).

The transitory part of blood nutritive system into the beginning lymphatic system is composed of queer looking filtrating glomerules. All blood capillaries contain amounts of red blood cells, which are organized in these transitory parts in something like minute blood clots. As far as the capilaries continue we find brush-like capillary fissures, intensely lightbreaking, which get along further in the capillaries or bend and turn in brightly illuminating capillaries of 10—20 $\mu$ in diameter. This glass-tube like empty vessel, bent in arches 50—70 $\mu$ long is filled up with a glassy transparent mass, the petrified haemolymph with rosy phosphorency in oblique light of microtechniques. A polygonal cell sometimes in form of a mutilated cone, divides the intermediate part of the filtration glomerule, thus regulating the outflow of filtrated haemolymph into lymphatic capillaries and farther on. This special cell is about 20 $\mu$ big, sometimes even bigger. [Tabul. No. XVII., fig. B. (c.) 9., (c.) 10, (c.) 11., (c.) 12.] and in oblique light microtechnique its plasma is cupped and rosy phosphorescing. In honour of P e t r b o k I called this celle after him (Petrbok's cell).

Haverse spongious bone system build up complicated structures of real bones secondly changed and recrystaled in calcit six-sided rhomboeders. Massive structures of spongiosa are reguarly gathered in two zones when diagonally broken.

The uppermost first part forms a thin layer represented by melted organic albuminoids (phosphoproteolipids, nucleoproteids, phosphoproteids, ribonucleoproteids), and has a golden-yellow colour in native microobjects. Staining is successful in methylene blue, eosin, Giemsa, methylene-green and argentaffine impregnations.

Strong beams in the second deeper layer consist of pointed rhomboeders and pynacoids in the form crystal drusen, directed in previous axes of pressure. Crystals of the outer basal layer just beneath the melted proteins are also coloured by all previously mentioned dyes, creating a many-coloured picture of brightly luminating rose, blue, and green and violet edged crystals.

II. B. (c.) — B. (d.) There are numerous blood sinuses among spongious bone beans, full of all kinds of cells of the reticulo-endothelial-erythrocyte branch. They are coloured yellowish brown and yellowish orange as blood plasma and blood cells do. Plasma of the haemoglobinogeneous reticuloendothelial cells and cell's nuclei of this developement branch is yellowish lemon-like, nuclei orange and amber. Reticuloendothelials are argentaffine and after reduction of metallic silver they are precisely contoured and with a fine network in cytoplasma full of holes (strainer-like). The nucleus in native preparates is bullous, of yellowish-amber colour, after being galvanoplastically silverized it turns bluish black with a prominence above the plan-convex sheath of cytoplasma. Edges of reticulo-endothelials are full of small wavy incisures, holding tightly the neighbouring cells one to the other in a continuous reticulo-endothelial tapetum of large epitheloid cells. (Tabul. XVIII. fig. B. (c.) 14., 15., 16., 17., 18.)

Easy breaking of these cells enables us preparation of microspecimens, where single petrified reticuloendothelials, can be studied.

Reticuloendothelials in the wall of blood sinuses have always a yellow cytoplasma sometimes finely granulated, their nuclei being orange or amber-yellow. Iron haemoglobin-like pigment is to be found both in cytoplasma and karyoplasma of these cells.

Reticuloendothelials belonging to lymphatic sinuses and capillaries are big as well (20 $\mu$), there plasma being gray and nuclei pitch black. That is how we can easily differ both of these reticuloendothelial groups in native microobjects.

Haemoglobinogenic reticuloendothelials are yellow as well as their nuclei. Enzymogenic reticuloendothelials are slate-gray with black nuclei. Their appearance is waxy, dull. Both kinds of those reticuloendothelials are argentaffine and their base is covered by a brushy edge. (Tabul. No. XVI. fig. B. (c.) 1., 2., 3., 4.. and Tabul. No. XVII. fig. B. (c.) 7., (c.) 8.) The amorphous blood plasma is lemon yellow, the amorphous mass of lymph is dull wax, slate grey and luminates in rose when obliquely light microscoped. (Tabul. No. XIX. fig. B. (c.) 24.)

Reticuloendothelial systems with oxide-reducting qualities contain a haemoglobinic breathing pigment (Fe.) dissolved either in plasma and nuclei, or finely granulated in erythroblasts (germinative red blood cells), farther in blood platelets and in the perinuclear area of the reticular cells, not yet differentiated in osteogenetic structures (osteoblasts, osteocytes).

Having lost their ciliary forming the haemoglobinogenic reticuloendothelials change in blood sinuses in germinative red blood cells (erythroblasts).

From these grow microcytes with small nuclei or without. After loss of nuclear masses erythroblasts also change in oval, lemon yellow corpuscles, filling arteries and arteriovenous systems of nutritive capillaries. [Tabul. No. XVIII. fig. B. (c.) 15, 16., 17., 18., and Tabul. No. XIX. fig. B. (c.) 19., (c.) 20., (c.) 22.]

Endothelial haemoglobinogenic cells transform farther into bone producing elements (osteoblast and osteocyt), losing their ciliary trimming and slowly getting covered by an amorphous bone substance.

Basic substance of bone lamels is lemon-yellow with multiple communicating bone cells cavities and dendritic network of cell communications inside. Plastimicroreliefs of cells and dendritic network appear after silver-impregnation. We see, how the former endotheloreticular-cell argentaffinity (mother form of osteocytes) has been preserved.

In the evolution of oxydoreductase system of haemoglobinogenic cells we can trace the descending concentration index of oxyhaemoglobine according to different staining of granules and plasma and nuclei. Lowering and raising of haemolympha concentration capillaries of enzymogenic evolution RES cells may thus be proved as well.

Oxydation of bone systems is being regulated by pericellular argent affine fissures, where there are fine networks on bordering regions of two medias. (Tabul. No. XV., fig. (c.) 5., (c.) 7., (c.) 8. Tabul. No. XVI., fig. (c.) 1. (c.) 4. Tabul. No. XVII., fig. (c.) 7., (c.) 8., Tabul No. XVIII. fig. (c.) 14.)

A similar oxydo-reductase system is represented by argentaffine network on borderparts of filtrating, brushlike glomerular divisions, where the haemolymph itself has luminiscent qualities after being reduced. Luminiscency is not solely produced by homogenised lymph, but even in the first 70 $\mu$ capillary transformating system's of haemolymphatic deconcentration to properties lymphatics. It can by proved in the first regulatory Petrbok's cell of this system. (Tabul. No. XVII. fig. B. (c.) 9., (c.) 10., (c.) 11., (c.) 12.)

After comparing two luminiscent colour effects a plausible explanation of functions of two systems can be obtained:

1. oxydo-reducing system haemoglobinogenic (Fe. pigment)
2. oxydo-reducing system enzymogenic in which the luminiscence of all its derivates may be proved (P.).

I have been able to find some other sac-like filtres in I—II—III grade capillaries (beside the mentioned brushy filters). Tabul. N. XXI. fig. B (d.) 12., 13., 14., 15 a, b. Tabul. No. XXII. (B.) (d.) 11.

These are afferent yellow coloured arterioles, immerging in microsacs in 3-5-7 in number. Just in renal glomerules these capillaries are ramified in these sacs too. The sac-walls are two-layered argentaffine, of cells almost 30 $\mu$ large. Haemolymph is filtrated by osmosis in these sacs and becomes luminiscent. The outflow from sacs is enabled by 1—7 capillaries into broader lympho-beds and the luminosity strengthens. (Tabul. No. XXIV. fig. B. (d.) 20., 21, 22., 23., 24., 25., — Tabul. No. XXV. fig. B (d.) 26., 27., 28., 29., — Tabul. No. XXVI, fig. B. (d.) 30., 31., 32., 33., 34., 35., — Tabul. No. XXVII, fig. B (d.) 36., 37., 38., 39., 40., 41., 42., Tabul. No. XXIII. fig. B. (d.) 16., 17., 18., 19., — Tabul. No. XX. fig. B. (d.) 1., 2., 3., 4., 5.)

According to different chemical characteristics we presume deep changes in molecular and nuclear systems Fe, P, O-N-H-He, S, C.

To different morphologic changes (being easily traced) belong also different functional adaptations of formerly neutral cell elements, which had been changed by adaptation and under influence of nuclear changes in space and time in harmonic quant systems of luminosity . . .

In sinuses of spongious bones neutral RES (reticulo endothelial system) cells are formed and here it is where they divide (differentiate) in lemon and orange yellow-microobjects. Here they differentiate in osteogenetic and erythropoetic ones.

Evolution of enzymogenetic cells (from neutral RES of appearance lipophages cells to granulocytes) takes place in closed lymph vessels and sinuses of cylindrical bones.

I have not been able to find a direct inflow of Haverses and Volkmann's capillaries in blood and lymph sinuses anywhere.

II. A. (c.) In histo-paleontologic materials the tube-like bones are a combination of cylindrical layers formed into simple or complicated Haverse-systems. Most of tube-like bones have infusory-like ended diaphyses (funnel-like).

Their appearance being sponsored by statical and dynamical changes in epiphyses, filled by spongious bone masses. The former middlepart

width of the cylindrical bones consisting of many cloak like cylindrical lamels narrows towards the epiphyses the number of fifteen layers being reduced to 4 or two layers. In places of reduction of the cylindrical bones spongious bones are formed, the beams of which arch the marrow cavity of cylindrical bones. These beams follow traction directions and thus strengthen the thinned parst of bones, substituting compact spongious bone-masses by light spongious railing. The bone thus gains on firmmess, lightness and elasticity by loss of compact.

The bone cavity enclosed a broken out medulla (marrow). Rests of this marrow are easily to be studied in individual parts of cavity which narrows proximally and distally forming saddle-like cascades of cavities widely communicating among themselves.

Whole cylindrical and spongious bones, including the cascade cavities were built up by interesting architectonics. Regularly distances osteocytes form stripes and fans of Heverse's systems. Bone block lamellae communicate not only through the capillary systems of Haverse and Volkmann, but through channels of nutritive capillaries, which penetrate the walls of tube-like bones obliquely into nutritive arteriols of the bone-marrow.

The bone marrow contains large epitheloid cells (20—40 $\mu$) with a waxy dull cytoplasma, absorbing light. It is finely granulated, with pitch black, bullons, oval nucleus. Cells are rather densely spread, some in argentaffine gray. The intercellular network is argentaffine as well.

These described large epitheloid cells in cylindrical bone cavities are mineraled some having on oval nucleus, some a kidney-like one. The largest cylindric bone cells (30 $\mu$) have pitch black nuclei 3—5 $\mu$ big. Small nuclei use to be in a finely granulated perinuclear area. .(Tabul. No. XIX. fig. B. (c.) 21., (c.) 25., Tabul. No. XX. fig. B (d.) 1., Tabul. No. XXI. B (d.) 7., 8., 9., 10.)

II. A. (d.) Osseus substance of tentorium cerebelli represents the former tissue brain covers which later ossified. This described part divided the central and dorsal fossa. This dividing part consists of two flat bones and a spongious bone amidst (diploe). Both formerly displaced. lamellae get nearer towards the insertion of tentorium cerebelli to os petrosum and finally confluat in one solid board.

Microscopical its structures is similar as in previous findings.

II. A (e.) Osseus substance from clivus Blumenbachii of the scull and the outer part of the flat bone. Between both of them is spongious substance highly vascularisated.

Brain capillaries and praecapillaries present an interesting finding when transiting from periost to the surface of brain gyres. Large cells supporting vessel walls are situated outside the leaving spot of capillaries from precapillary beds. They remember us of large pericytes, which normalise the puls rhythm of vessels beside supporting them. There is melanine pigment in many RES and endothelial cells belonging to cerebral vessels.

II. (C.) I have not been able to find fibrocytes (an important part of mesoderm) currently. They form only in perivascular tissues an adventitial, not differentiated meshwork of oat-like, yellow cells.

It is impossible to describe and distinguish tissue cells and muscle cells from vessel walls, as their is no difference between them.

An argentaffine network coating covers perivascular lymph. Spaces in sleeve-like forms, embracing the main arteriovenous beds and collaterals emerging from these as well. (Tabul. No. XXVIII. fig. C. (a.) 1., 2.)

II. (C.) a. When studying macro-specimens No. IV. from skeleton muscles, bones, tendons and bursae mucosae I made many microrelief reprints. Objects thus obtained had been studied in oblique light microscopy techniques and I found note-worthy microscopical differences among tendons, periost and transversely striped skeleton muscles.

By dividing single zones I gained reprints of various layers of these. After finishing with petrificated layers I gained fine undulated impressions of intermuscular septs, which looked like pictures of flat fascia. (Tabul. XXVIII, fig. (a.) 1., 2., 3., 4.)

A further important finding includes fibrillar myxomatous ligaments, a main part of periarticular ligaments near bursae mucosae. Pieces of bursae mucosae walls have been obtained from microscopical petrified skeleton muscles, bones, tendons and formerly thin ligament. The sac wall is about 2 mm. thick and brightly glistening. The inner surface of these cavities is finely granulated, granit gray. Brown stripes penetrate the whole sac wall, from the outer surface. Cavities are found in the size of acorns (formerly interpreted as such) and remember us of hazelnuts on the breaking point. They are systematically arranged between the bone and neighbouring skeleton muscles, which has been abrupted and that is how these cavities can be freely studied. Their dimensions: 14 X 10 mm., 9 X 6 mm., 18 X6 mm., 16 X 10 mm., 20 X 10 mm. and 10 X 6 mm. of length and depth. They offer us an interesting finding of mineral materials. Walls of bursae mucosae are composed of three kinds of crystals. The innerest part is grayish brown, cleanable with chloroform and xylol in slaty-gray, having been an endothelial layer of these mucous-forming sacs. Here it was from where the crystallisation started, throughout till into neighbouring myxofibromatous ligaments. The sac walls are soft and mucous, their substance forming gliding materials for articular and periarticular spaces there, where stronger tractions and pressures could dammage. The mechanically exposed soft articular parts of locomotion. These structures being rather fluid and gelly, are without a firm organisation.

All chemical substances of these sacs changed by metamorphosis in hard unusual crystalled cell combinations.

The sacs walls have roughby counted three layers of bright crystals. The first one are rhombohendrons, forming a structure of support.

The second layer contains slender long scalenoheders beginning among the crystals of the first layer of support.

The second zone crystals are saw-like and stool-like. The periferal third zone is from atypical six sided rhomboheders, penetrating both previous layers and shows as calcit polarisating might—islands characteristics where crystals get bent. Most numerous bending deformities are in place, where crystal pressures have been the mightest and here

is where calcit gets characteristics polarisatione one. (Tabul. No. XXIX. fig. C. (a.) 5., (a.) 7 a, 11, a—b. Tabul. No. XXX. (a.) 14.)

When carefully studied we find gentle, web-like fibres in axes of all three kinds of these crystals forming a net of guirlandes. And pitch black spots hang on this net, looking like children toys (Tabul. No. XXIX. fig. C. (a.) 9., (a.) 10., (a.) 11., tabul. XXX. fig. C. (a.) 12., 13., (a.) 14., (a.) 15.) Fig. No. 4.

These are pitch black nucleus rests, variously bent, fixed on fibromyxomatous tissue remnants. The nuclei are different size because of their different bending in space. In oblique light microtechniques they have their own shadow and a cast one, doubly, contoured in polarisating calcit islands-like. The inner endothelial layer of bursae mucosae is flat and cubic, built up of fibroepitheloid cells with a graphite gray plasma and pitch black nuclei. This innerest part is argentaffine.

II. (C.) a. Transversely stripped skeleton muscles gave desired structures in microrelief slides and I had to search long for transverse stripping till some single petrified muscle fibres on bone fragments could be found. Here the fibres either attached, or produced a flat relief with transverse stripping when touching the bone. (Tabul. XXVIII. fig. C. (a.) 2., (a.) 3., (a.) 4.)

Skeleton muscles form three exactly different plastical groups on macroscopique specimens, as we shall see further on.

As far as here I have been able to determine important tissues and cells of the first and third germinative leaf, obtaining thus a rich material to be studied. These cells are well conserved, having changed in space and time their biologic organic structures into anorganic substances. The cels are fine structures of a gentle beauty. Sometimes transparent as glass in many shades ranging from yellow to orange red. Also the gray and dull colour, up to the pitch black has its original colour. Characteristical for former organic substances is luminosity of lymph and haemolymph, which witness the luminosity characteristics of substances before 70.000 years. We shall try to investigate this important effect in another communication. Luminosity of mineral substances in crossed Nickols states various transformations of calcit, which presents about 140 various atypical crystal modifications in the studied material.

I complete the paleohistological findings by adding a brief description of macroobjects and their syntopic relations.

Petrified brain No. I., macrofoto Tab. XXXI. with cerebellum and a part of neck spinal chord have a transverse diameter of 155 m., height from clivus Blumenbachii 95 mm., bitemporalis width 110 mm. The sole brain, well preserved has 140 mm. measured from polus frontalis to the attachement sulcus of previous tentorium cerebelli. Cerebellum measures (its length) 35 mm. above the convexity of vermis cerebelli.The protruding part of spinal chord measures 10 mm. to the point of breaking. The left cerebellum hemisphere measures 25 mm. from the mouth of sinus petrosus superior. In the triangular space between temporal-occipital brain lobes is at the transitory point of left hemisphere convexity an irregular rhombic sinking, directed towards the brain base along the left part

(ramus) of the occipital bone. This rhombic sinking originated by fragmentation of pneumatised cells in the mastoid process of the left temporal bone. The breaking happened on the border line of sutura occipitomastoidea et sutura parietomastoidea lat. sin. Cell impressions are easily traceable in the abrupted left zygomatic process, where a horizontal semicircular channel of the vestibular organ is to be seen. Just underneath

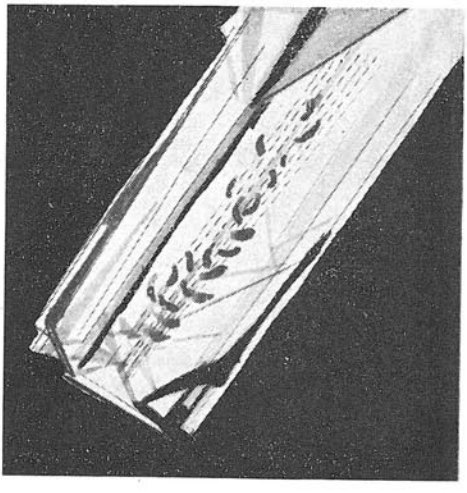

Fig. 4. Krystal dvojlomného vápence s osovou krystalisační mřížkou, která obsahuje myxofibromatosní buňky a jejich jádra.
Crystal of double refracting calcit with a web-like fibres in axes containing myxofibromatous cells and nucleus guirlandes.

is a broken trunk of the posterior cerebral artery and a plattened left sigmoideal sinus. The left temporoparietal part is covered by one third with rests of fossified vitreous lamina ossis temporalis et ossis parietalis. Remaining two thirds of this zone are without a bony cover. The brain substance is yellow in these places, sometimes spoiled by corrosion, to that under the thin layer of coloured brain part a white, finely granulated substance appears, which spoils the smooth covering areas in 40 by 50 mm. width. A plaster of Paris similar crumbling substance originated by metamorphosis of the gray brain substance.

The yellow membranaceous brain covers are about 1½ mm. thick and preserved towards the upper sagittal sinus. Left styloid process appears to be a 9 mm. long bone rest under the fractured part of the left mastoid process. Facies cerebrals of the left temporal bone squama is covered with bone rests of lamina vitrea many apertures for branches of the left cerebral medial artery.

The left temporal lobe and the region of the left lateral cerebral fissure are damaged in an area 73 mm. by 30 mm. by deep corrosions. Here the fossilified brain cortex changed in white plastery powder 6 mm deep and also here the grey substance, of a lasture-like breaking.

The same happened to the left olfactory tractus and left orbital gyrus. The left frontal inferior gyrus is devasted by one half, the left frontal medial gyrus by one third and the superior part of the gyrus frontal. super. is devasted up to gyrus centr. ant. sinister.

There are several white surface corrosions of the sinus sagittalis sup., which is otherwise easily followable for 90 mm.

Redbrown corrosion spoiled the gray brain matter as well as the white brain matter into the depth of 9 mm. higher. Sinus sagittalis sup. is in area 5 mm. wide 3 mm. than the surrounding tissue. The brain surfaces are as bright as the neighbouring parietal-occipital gyres of both brain hemispheres.

We can roughly calculate with a little damaged left brain hemisphere, cerebellar hemisphere and the left part of spinal chord down to the lower olivar nucleus. But for a little corrosion of all three temporal lobes 55 X 50 mm., which spoiled their gray matter, is the right brain, cerebellar and spinal hemisphere almost intact. There is a gap in the right lateral cerebral fissure 27 mm. wide, so that a red brown corrosion may be studied 5 mm. wide and 10 mm. deep among the gyrus front. sup. dx. and gyrus central. ant. The rough part laminae vitree of the frontal bones forms a prominency above the superior sagittal sinus with Pacchioni granulations, full of blood capillary beds. The right mastoid process is again typically abrupted at the sutura occipito-mastoidea lat. dx. and sutura parieto-mastoidea dx., so that we can study the semicircular superior channel and the first cochlear winding. Tympanal antrum is widely open.

Brain gyres of the frontal, parietal and temporal region are plastic and the sulces are visible. Left olfactory tractus is absent. The right olfactory is spoiled by a white corrosion but for a 15 mm. rest of the right olfactory nerve tract, which lies between the orbital and rectus gyres. This preserved rest of the right olfactory tract from an oval, longitudinal prominency towards the optical chiasma.

From the brain convexity No I. we get to the description of the brain base, 87 mm. long from the frontal pole to foramen occipitale magnum, herefrom via the Varoli bridge to the begin of spinal chord are another 55 mm.

From the right olfactory tract region we get from the anterior skull fossa to a staircase-like hollow, where the optic fascicles enter both sides immerging into the middle brain on both sides of the turkish saddle after deccusation.

The right optic tract is 15 mm. long and 5 mm. wide. The left one is almost totally abrupted, measuring 5 mm. before the chiasma.

The small wings of the left sphenoidal bone is broken off too. The right small wing of the right sphenoidal bone is preserved sphenosquamous suture. The sphenoidal bone body is transversaly fractured. Both the big and small wing of the left sphenoidal bone are missing and the anterior clinoid process is abrupt but easily localisable. The facies temporalis of the left sphenoid is broken off together with the temporal pole of the left brain. Hehe we see a funnel like hollow 13 mm. deep. On the proximal ceiling are rests of spongious bone from the orbital crist.

Gentle spongious bone frame-work forming the sphenoid body continues directly into basilar occipital body at the sphenoidoccipital suture. The important tubercle belongs to the cortical layer of the basilar bone and to the spongious diploe. The cortical bone is 3 mm. in strength

and yellow, the diploe is red brown, so that both parts can be easily distinguished.

Both rami of the occipital basilar part diverge obliquely and shape a V-like former and side part of the big occipital foramen from the pharyngeal tuberculum. The right branch of the basilar part continues into the occipital condyle, damaged by the abrupted articular facet. The fracture of the bony occipit. directly continues with the previously mentioned fracture of the left mastoid process. The mastoid margin fenestrated after abruption of the upper semicircular channel and with the first cochlear winding opens above it.

Cerebellar hemisferes descend roof-like symetrically on both sides and is not hidden under the occipital cerebral lobes. We are able to follow both occipital sinuses and a convex 15 mm. long part of the vena magna Galeni from the cerebellar tentorium insertion, which divides the cerebellar tissue from the brain. Rests of spongious frame-work covers the surface a bright layer of cerebellar coverings (dura mater) can be seen where the cerebellar gyres and vermis rise. The transition to neck spinal chord is oblique. Many reddish brown errosions in places of big vessels demonstrate the beds of big spino-ponto-cerebellar arteries. There where the left posterior cerebral artery dives between the occipital lobes and between the insertions of the left cerebellar tentorium is abrupted the left cerebellar floccullus. Here is a crater 20 mm. deep with simultaneously missing left brachium pontis. In the same place of the right side is a flattened hole of the abrupted right spinal artery.

On the transverse fracture of the neck spinal chord are corroded vessels with rusty contents. They immerge from the outer spinal covers into the white and gray matter of the neck spinal cord where both lower nuclei olivares are stated.

The right cerebral hemisphere being narrower than the left one, we can easily observe an asymmetry not of the brain alone, but also of the little brain and spinal cord. We can accept the opinion that this marked difference arose when mineralisation of the white and gray brain matter took place inside the lateral ventricles, where the brain is mostly devasted.

Brain No. II. macrofoto Tab. XXXII. measures in medial line from the cerebellar tentorium insertion to the right cerebral frontal pole 230 mm. What was left over from the left hemisphere measures 50 mm. from falx cerebri to the frontal middle gyrus on the biggest convexity. The deformed right hemisphere measures on the biggest convexity 60 mm., the rest of 55 mm. to confluens sinuum is divided among cerebellar and spinal rests. The anterior brain fossa counts 55 mm. from the right frontal pole to the deformed part of the right sphenoid body. Here remain 110 mm. to the broken end of the spinal cord in medial line.

Left cerebral and cerebellar hemisphere including the neck spinal cord are rather spoiled. We can roughly determine the left central sulcus, which divides the defective frontal gyres from the spoiled temporal ones.

Cerebral lobe tissue has been substituted for a sandy calcium sinter. The same has happened to cerebellar tissue and spinal cord, substituted in the posterior fossa for a granular sandy trapeze mass. The right brain

hemisphere is less devasted. The right frontal pole is transversely deep fissured. The surface of the convexity, of the side parietal and temporal and occipital gyres is deeply corroded. The right cerebral hemisphere is substituted for a hard stony mass from the cerebellar tentorium insertion.

Near the localisation of the inferior temporal gyrus the middle brain fossa is covered by a brownish yellow bone 10×25 mm. and underneath this lamella we find a displaced fragment of the basillar part of the occipital bone.

By the fracturing of the occipital bone body the topographic structure of the cranial base as well as of brain had been spoiled. After the fracture the masses of middle brain, pontis Varoli, medullae oblongatae and spinalis were pushed as the vertical pressure directed them and were followed by left dislocation of already petrified fragments.

From these findings we may deduce a total deformation of cerebrum, cerebellum, medullae spinalis et oblongatae after a previous petrifying period when new consolidation, rather complete, has followed.

In places of white corrosions the grey brain matter has been transformed in a white dusty sand. All other parts of this macroobject are pigmented dark brown. Thin bone lamellae of the vitreous laminae are yellow changing into grey.

The spinal macroobject with a petrified spinal chord No. III. (Tab. XXXIII) contains three whole vertebras, a half of the fourth and a quarter of the fifth one. The fourth vertebra is displaced, but the fifth resumes its position.

Vertebral bodies are heavily corroded and full of crooked transverse and oblique corridors with fine rusty dust inside them. These are petrified rests of vessels, well demonstrable on the yellow part of the spinal column turned towards the body in vivo. There are morphologically changed and damaged transverse processes. Spinal vertebral processes are flattened and deformed on the convex side, with their ends covering proximal parts of neighbouring vertebra. The convex side of this specimen is grayish brown and very corroded.

This described spinal portion reminds us of lumbal vertebral badly deformed by corrosion. Single vertebral bodies had been petrified and united. There is a transverse fissura 2 mm. long on the cross fracture of petrified vertebrae, similar to a plattened ellipse. On the other side of the fracture this fissure measures 10 mm. A thin wire sond can be pushed 10 mm. inside these fissures.

The previous spinal tube (canalis spinalis) is filled up with a sandy yellow crumbling mass. When studied microscopically we gained a rich histological material of all kinds of ganglion cells, microglia, oligo and astrocytoglia.

Macroobject No. IV. (macrofoto Tab. XXXIV.) contains petrified skeleton muscles with bone insertions plastically modelled even with fasciae and mucoses sac. Characteristics of these bone fragments are those of spongious bones. The largest one acts as muscle carrier. Major part of this bones is crumbled, so that a wide cone gap appeared after descriptive addition and plastical model of bone rests and muscles we get an upper past of bone diaphysis continuing in the epiphysis. The

upper apperture is 105 mm., the lower 90 mm. After abruption of the bone wall the muscle masses bulged and fill 9/10 of the described object. These wedge-shaped muscle masses measure on the upper area 50 mm. diagonally and in the lower area 30 mm.

A visible plastical part of muscle hides behind the bone tapetum in the width of 35 mm. On the lower end of this bone tapetum muscles measure 10X12 mm. This whole described part is melted to the outer surface of the main carrier bone No. 1.

A deep gap divides the pyramidal muscle from the second muscle belly which forms the outer part of this muscle group.

The second muscle body is 5 mm. wide near to the base of the muscle pyramide No. 1. Muscle No. 2. is 73 mm. long and there where the pyramidal muscle hides behind the osseous tapetum his oval part measures 13 mm.

Both muscles are parallel, being connected by a common tendon sheath, which dives between them and so divides them as an inter-muscular sept as well. This sheath we may characterise as a perimysium, transitory to the periost of the spongious epi and diaphysis.

A characteristical picture may be seen on the lower surface of No. IV object.

The lower ends of both described muscles No. 1. and 2. form two semicircular plastical curvatures. The inner arched part relaxes in a halfsinusoid on the periost of the main carrier bone No. 1. The outer survature of the second muscle slowly descends to the mineral tissue of peculiar microscopy characteristics.

Surface of this place contains a fine framework of metamorphosed travertine of triangular shape. The inner side measures 70 mm., the upper 75 mm. and the base 55 mm., connecting both previous ones. Here we find cavities forming a functional anatomical unit. These cavities are separated by thin septs from former tissue. Their contents are about 3 cmc. They are empty looking like a longitudinally parted hazel-nut or acorn, and that is what we had put them for at the first moment. The cavity walls are 2 mm. thick glisten and break the light rays with a crystal glitter when cleaned. The inner surface of these cavities is granulated, greyish yellow with brown stripes, which can be traced through the whole wall till to the outer surface. These cavities form a unit connected with No. 1 carrier bone. Farther interest has been devoted to the irregular trapeze, the arms of which measure 25X23X10 X18 mm. It is a diagonal fracture of No. 2 bone, functionally connected with the first bone. No. 2. bone has its cortical layer trimmed by a brownish zone. The longer part is obliquely turned to bone No. 1. and supports two transversely broken muscles, already previously described. The side bone lamella is corroded, the inner lamella concave and from here on starts a small piece of petrified tendon, of brownish colour. This tissue membrane is infracted in -V- shape and its inner duplicature returns to the edge of obliquely fractured bone No. 1.

No. 2 bone is cross-fractured, filled by a sandy,, yellowish white powdered mass of bone spongiosis and marrow. The brownish trimming

(of the tissue membrane) continues in a notched line on the lower surface of the same bone and gets on to bone fragment No. 3.

No. 3 bone hangs with its brownish trimming together with the cross-fractured hollow bone No. 2. It is a longitudinally broken long bone. Its inner wall measures 60 mm. of length, the lower wall 40 mm. and 10 mm. thick. Between both slices of compact bone is the bone cavity full of spongious frame-work and marrow. Both ends are 33 mm. wide.

Colour of the inner lamella is brownish yellow in its whole course. The marrow colour after polishing is yellow, the outer lamella colour is yellow with orange.

All three bones formed a sort of unity. I return to the description of two muscle bundles according to the unity of bones No. 1, 2, 3, and finish by describing a muscle bundle No. 3.

On the highest convexity of No. 1. bone is placed the third muscle bundle, plastically modelled in halfconvex surface. On cross-section it has ellipse-like contours 10×15 mm. and lies on the inner surface of the pyramide muscle. From the surface inwards lies a diagonal incisure under which the muscle is convex once more. Farther on the muscle fibres grow stronger. 20 mm. from the upper surface the muscle broadens, so that it measures 15 mm. from the border inscisure of the pyramid muscle, dives behind the mass of carrier bone No. 1., which is here about 20 mm. wide.

A cavity 17×15 cross fractured and filled muscle fibres of No. 3. muscle between the bone and neighbouring petrified substance. The cavity is freely open between No. 3. muscle and the epiphysis spongia.

Underneath it and 25 mm. far off is one more cavity, similar to the five already described. The sixth cavity has the following dimensions: 13×10×5 mm. anteroposteriorly is the wall faded. The outer wall after having formed a sinus measures 13 mm. Rough outlines of this described complex may be followed on the upper surface of the specimen. In furrows, separating individual fields are meandering channels full of rusty powder. These are petrified vessels hidden in intermuscular septs which divided single functional wholes and to these bone fragment No. 4 also belongs.

The spongy bone No. 4. has a particular set in the described block. It runs from the upper fractured area of the whole macroobject and reaches the lower surface of this same object by its lower fractured end. It is sabre-like curved as far as we can follow.

The bone area is abrupted in about 20 mm. from the four cavities. From the upper surface of this described cavity run along its side walls ramificated channels, vessels full of rusty powder. They wind along the outer surface of this mentioned cavity and along the upper surface of this block they join as a rusty tissue sept the down part of the fraction-area, to the sabre-like bone No. 4. Many differently twisted vessel channels with rusty filling run in arches from the outer surface back to the fractured tube bone No. 3.

This is the description of topographical connections of single bone fragments, skeleton muscles, tendons, ligaments and intermuscular septs and of systems of little cavities.

This complete macroobject No. IV. of the static and dynamic bone block, of skeleton muscles, tendons and synovial mucous burses is from a physical point of view a synthesis of all locomotion group, which had been parts of an important joint (of a thoracal limb). Main carrier bones had been broken in upper parts of diaphysis there, where their muscles and fasciae were connected with mucous synovial sacs.

I was glad to complete the first part of the studied material by this brief communicatiou, which broadened our histologic knowledge and presented further possibilities in histologic investigation of microscopic petrified structures.

SEZNAM LITERATURY:


1. H. GODWIN: Plant Biology. Cambridge University Press, 1939.
2. W. J. HAMILTON M. D., J. D. Boyd M. A., H. W. MOSSMAN: Human embryology (Heffer) Cambridge 1947.
3. PASCUAL JORDAN: Anschauliche Quantentheorie, Berlin Springer 1936.
4. C. CLAUS, GROBEN, K. A. KÜHN: Lehrbuch der Zoologie (Jul. Springer), Berlin—Wien 1932.
5. HORST WERNER MATTHES (Halle/S.): Der gegenwärtige Stand der mikropaläontologischen Forschung. Forschungen und Fortschritte 31. Jahrg., Heft 2. Berlin, Februar 1957.
6. JAR. PETRBOK: Měkkýši slovenských travertínů. Sborník Státního geologického ústavu československé republiky, Vol. IV, 1924.
   JAR. PETRBOK: Měkkýši slovenských travertínů, Sborník Stát. geologického ústavu československé republiky, Vol. VI, 1926.
7. HERMANN SCHMIDT (Göttingen): Cornberger Fährten und Geschichte der Reptilien. Forschungen und Fortschritte, 31 Jahrg., Heft 8. Berlin, Febr. 1957.
8. O. ŠTĚPÁNEK: Pleistocenní želva bahenní z travertínů v Gánovcích. Časopis Šafaříkovy společnosti, Bratislava VIII (3) 1934.
9. HERWEY W. SHIMER and ROBERT R. SHROCK: Index fossils of North America. Technology Press Massachusets Institute of Technology. (John Wiley Sons) New York 1947.
10. H. J. SCHERER: Vergleichende Pathologie des Nervensystems der Säugetiere. (Georg Thieme Verlag. Leipzig 1944.
11. F. PRANTL: Život českých pramoří, Čs. Akademie věd a umění 1952.
12. JOS. SAHÁNEK: Vznik světla v plynech. (Jednota č. matematiků a fysiků) 1941.
13. EMAN. VLČEK et alii: Nález neanderthalského člověka na Slovensku. Slovenská archeologie (Slovenská Akademie věd, Bratislava). Vol. I., 1953.

TABUL. No. V.

fig. 1. (a.) I. — Chlup podél z fosilikované, sklovitě průsvitné základní hmoty. Hair of fossiled, glassy transparent hommogenous mass. (ex errosionibus tractus olfactor. cerebri No. I. (Gánovce).

fig. 1. (b.) I. — Chlup objemnější předešlého na koncích zlomený, rozdělený na čtyři podélné pásy, na lomu tvoří podkovitou kresbu. This hair is broader than the above-mentioned one. The ends are braken off. On the hair fracture we can distinguish four stripes in the form of light breaking circles, which remind us of horse-shoes (ex errosionibus tractus olfact. cerebri No. I.).

fig. 1. (c.) I. — Chlup s míškem (folliculus pili) po délce zvlněný. Hair with a follicle, shaped bulb-likely (ex regione chiasmatis nn. optic. cerebri No. I.).

TABUL. No. VI.

fig. 2. (a.) I. 1. — Polyedrické gangliové buňky (cca. 10 $\mu$) s ulomenými neurity i dendrity. Small, polyedriques cells (cca. 10 $\mu$) without neurites and dendrites (ex tract. olfact. cerebri No. I.) Gánovce.

fig. 2. (a.) I. 2. — Polyedrické gangliové buňky (cca. 10 $\mu$) tvoří dendritickou plsť. Round, small cells and polyedriques cells ganglionares form meshwork of dendrites (ex tract. olfactor. cerebri No. I.).

fig. 2. (b.) I. 3. — Gangliové buňky (15—20 $\mu$) trojúhelníkovité s perinukleárním dvorečkem, někdy i se dvěma jádry. Ganglionares cells (15—20 $\mu$) sometimes triangular with clearer perinuclear area. Nuclei vesicle-like sometimes doubles (ex reg. gyror. temporal.) cerebr. No. I.

fig. 2. (b.) I. 4. — Gangliové buňky (15—20$\mu$) s tygroidní hmotou v cytoplasmě. Ganglionares cells (15—20 $\mu$) with tygroid substance in cytoplasm (ex corrosion. parietooccipital. cerebri). No. I.

fig. 2. (b.) I. 5. — Gangliové buňky 15—20 $\mu$ polyedrické s tygroidní hmotou v cytoplasmě. Ganglionares cells (15—20 $\mu$) with tygroid substance in cytoplasm (ex errosion. gyr. centr. cerebri). No. I.

fig. 2. (c.) I. 6. — Gangliová buňka se dvěma jádry, typu pyramidové (30 $\mu$). Big cells, over 30 $\mu$, nuclei vesicle-like, the tygroid substance light breaking, sometimes pyramidal type (ex ponte Varoli cerebr. No. I—II.

fig. 2. (c.) I. 7. — Gangliová buňka s granulovanou cytoplasmou se dvěma jádry, typ pyramidový (30 $\mu$). Big cells over 30 $\mu$, nuclei vesicle-like, the tygroid substance light breaking, pyrahidal type. (ex ponte Varoli cerebri No. I.) Gánovce.

fig. 2. (c.) I. 8. — Skupina gangliových buněk (30 $\mu$) s dendritickou a neuritickou texturou. Group of ganglionares cells (30 $\mu$) with neuro-dendritiques meshwork (ex ponte Varoli) celebri No. I.

fig. 2. (c.) I. 9. — Skupina gangliových buněk (30 $\mu$), polyedrických, s texturou dendritů a neuritů. Group of ganglionares cells (30 $\mu$) with neuro-dendritiques meshwork (ex ponte Varoli) cerebri No. I.

TABUL. No. VII.

fig. 3. (d.) I. glia 1. — Neurogliální plsť s četnými gangliovými buňkami. Neuroglial mesh-work with fragments of ganglionare cells (native material of spinal cord No. III.).

fig. 3. (d.) I. glia 2. Oligodendroglia po impregnaci $AgNO_3$.
Oligodendroglia cells silver-impregnated (ex reg. gyr. temporo-parietal, cerebri No. II.).

fig. 3. (d.) I. glia 3. Dendrogliální textura s krevní kapilárou.
Texture of dendroglia with fragments of capillary (ex spinal cord. No. III.).

fig. 3. (d.) I. glia 4. Oligodendroglia míchy po impregnaci $AgNO_3$.
Oligodendroglia silver-impregnated (makroob. No. III.).

fig. 3. (d.) I. glia 5. Inkluse gangliových a gliálních buněk ve dvojlomném kalcitu.
Ganglionares and glials cells included in crystale-calcit with double refraction (ex cerebr. No. II.).

fig. 3. (d.) I. glia 6. Oligodendroglia z mozku č. II.
Oligodendroglia from brain No. II.

fig. 3. (d.) I. glia 7. Oligodendroglia po impregnaci $AgNO_3$ z korose temporoparietálních laloků mozku No. II.
Oligodendroglia cells silver-impregnated (ex corrosion. gyr. temporo-parietale) of brain No. II.

fig. 3. (d.) I. glia 8. Rosetovité seskupení oligodendroglie impregn. $AgNO_3$ (z mozku No. I. gyr. central).
Oligodendroglia cells accumulated rosette-like silver-impregnation (brain No. I).

TABUL. No. VIII.

fig. 4. (e.) I. 1. Nervová vlákna s myelinovými obaly a s Ranvierovými zářezy a křížovitou strukturou světelného lomu.
Neuraxon with myelin covers and Ranvier's incisures (ex spinal cord macroob. No. III.).

fig. 4. (e.) I. 2. Nervové vlákno s myelinovou pochvou z míchy (natívní).
Neuraxon covered with myelin (spinal cord makroobj. No. III.).

fig. 4. (e.) I. 3. Gangliová buňka v kalcitu se dvěma neurity.
Ganglionare cell bidendrited (in crystal of calcit).

fig. 4. (e.) I. 4. Gangliová buňka se dvěma neurity (impregn. $AgNO_3$).
Ganglionare cell bidendrited (impregnated $Ag\,NO_3$) gyrus centr. cerebri No. I.

fig. 4. (e.) I. 5. Úlomky velkých gangliových buněk s neurity i dendrity inkludované v kalcitu.
Fragments of large ganglionare cells, included in calcit (spinal cord No. III.).

fig. 4. (e.) I. 6. Velké gangliové buňky s dendrity (paralelní uspořádání neuritů vtmelených do silné kalcitové destičky).
Large, polyedriques ganglionares cells with parallel arranged dendrits (gyr. parietalis et tract. olfact. cerebri No. I.).

fig. 4. (e.) I. 7. Velká pyramidová buňka se zdvojeným neuritem z gyr. central. cerebri No. I. (impregnovaná $AgNO_3$).
Large pyramide-like cell, bidendrited, silver-impregnated (ex gyr. central. cerebri No. I.).

TABUL. No. IX.

fig. A. (a.) 1. II. oss. Deskovitá kost z vějířovitě položených lamel.
The flat bone forming fans (ex clivus Bdumenbachii).

fig. A. (a.) 2. II. oss. Příčný zlom šroubovitě uspořádaných desek s kapilárou.
Transversal fracture of spinal arranged plates with central capilainy (bone No. 3. makroobj. No. IV.).

fig. A. (a.) 3. II. oss. Příčný zlom šroubovitě vinutých desek s centrální kapilárou.
Transversal fracture of bone layers with central capillay (bone of makroobj. No. III.).

fig. A. (a.) 4. II. B. Paralelní uspořádání arteriol v deskovitých kostech s kapilární šikmou spojkou.
Blood capillaries of the artery-venous system pararerly arranged in flat bones.

TABUL. No. X.

fig. A. (a.) 5. II. oss. Kostní buňky po impregnaci $AgNO_3$ s mnohočetnými jemnými výběžky.
Osteocyt's cells silver-impregnated (regio sellae turcicae) cerebr. No. I.

fig. A. (a.) 6. II. oss. Příčný zlom novětvořenou kapilárou vytvořenou ze dvou endothelií v ploché kosti.
Transversal fracture of native capillay formed two endothelial cells (flat bone).

fig. A. (a.) 7. II. oss. Plochá kost z protisměrně vrstvených vějířů.
Bone tissue forms fans sometimes diversed.

fig. A. (a.) 8. II. oss. Příčný zlom novotvořenou kapilárou z velkých retikuloendothelií v deskovité kosti.
Transversale fracture of neogenne capillary formed of large reticuloendothelial cells in flat bone.

fig. A. (a.) 9. II. oss. Isolovaná reticuloendotheliální buňka s hrubými plasmatickými výběžky přisedlá na kost.
Reticuloendothelial single ciliated cell fixed on flat bone.

TABUL. No. XI.

fig. B. (b.) 1. II. arter. ven. Kapilární endothel s řasinkovým lemem, tvořícím na basis jemné zoubky.
Endothelial cells with brush-like odges forming on the basis teeth-like pictures.

fig. B. (b.) 2. II. arter. ven. Kapilárv s buničným obsahem uvnitř.
Capillaries with cellulare contents (flat bone).

fig. B. (b.) 3. II. arter. ven. Velké artérie helicinního systému, které před rozvětvením mají v mateřské tepně svěrač (sfincter).
Larger arteries of helicin type with sfincter from circular cell-rings.

fig. B. (b.) 4. Rovnoběžné kapilární anastomosy v plochých kostech.
Capillaries anastomosis parallelly arranged on flat bones.

TABUL. No. XII.

fig. B. (b.) 5. Artérie II. a III. typu helicinního po spojení dvou artérií tvoří hadovitě vinutý společný kmen na přechodu z kosti do periostu.
Larger second and third grade arteries resembling us of helicine between muscles, periost and bone (flat bone of skull cerebri No. I.).

fig. B. (b.) 6. II. arter. ven. Teleangiectatic aneurysma (vak), ve kterém končí arter. helicina, z níž v dalším průběhu vychází kapilára.
Artery ectatic blood-sac (aneurysma) longitudinally eliptical above bone surface, between muscles, tendons and bone.

fig. B. (b.) 7. II. arter. ven. Kapilární odstupy arteriol z hlavního kmene tepny desátého řádu na rozhraní svalů, šlach a kostí.
Arteriol rammification of the artery trunc $X^0$ between muscles, tendons and bones (makroobj. No. IV.).

fig. B. (b.) 8. II. arter. ven. Systémy vakovitých výdutí (aneurysmat) na šestí kapilárních anastomosách.
The blood reservoirs (aneurysma) betwen six capillaries anastomosies.

fig. B. (b.) 9. II. arter. ven. Vidlicovité větvení kolaterálních arteriol v plochých kostech lebečních.
Forked capillaries in flat bones of skull (tentorium cerebelli) cerebri No. II.

TABUL. No. XIII.

fig. B. (b.) 10. II. arter. ven. Systémy kapilár na přechodu z epifýzy do diafýzy v houbovité kosti. Systems of capillaries between epi-diaphysis in spongious bone (macroobj. No. IV.).

fig. B. (b.) 11. II. arter. ven. Artérie Haversova systému v houbovitých kostech. Capillaries Haverse's system in spongious bones.

fig. B. (b.) 12. II. arter. ven. Šikmý průběh Haversových arteriol. Oblique course of Haversian's capillaries in spongious bone.

fig. B. (b.) 13. II. arter. ven. Odstup artérie Haversova systému a spojení se silným kmenem arter. typu Volkmannova. Kráterovité uspořádání kostní hmoty v místech zanoření tepny do kostního trámce. Haverse's and Volkmann's capillaries, crater's arrangement of bone for nourish channel (macroobj. No. IV.).

TABUL. No. XIV.

fig. B. (b.) 14. II. arter. ven. Zpětný odstup artérií uzávěrových systémů s velkými endotheliemi v místech kapilárního větvení. Blood capillaries returning agoinst the blood-flow. Blood vessels are mostly running in various directions.

fig. B. (b.) 15. II. arter. ven. Velká endothelie ve stěně odstupující arterioly (vpravo). Large endothelial cell on the wall of a tractured arteriol. (on right).

fig. B. (b.) 16. II. arter. ven. Obloukovitý přechod velkých cév z periostu do přímého kmene arter. typu Volkmannova. Circural transition of large arterioles from the periost to the capillary systems of Havers and Volkmann's type.

fig. B. (b.) 17. II. arter. ven. Vakovitě cylindrické aneurysma nad sfinkterem před odstupem kolaterálních kapilár. Aneurysmatic sacs arteriol, above the sphincter before the ramification of capillaries between muscles, tendons and bone (macroobj. No. IV.).

fig. B. (b.) 18. II. arter. ven. Uzávěrové endothelie na stěnách odstupujících kapilár. Closing endothelies on the walls ramificated capillaries.

fig. B. (b.) 19. II. arter. ven. Přeslenovité větvení odstupujících arteriol z arterie a zpětné vinutí helicinních arteriol. Ramificated arterioles helicines running back from the mather artery. (microobj. No. IV.).

TABUL. No. XV.

fig. B. (c.) 1. II. RE. Retikuloendotheliální buňky na stěně sinusu zanořeny kartáčkovitým lemem ku první řadě osteocytů. Reticuloendothelial cells brushes, immerging in bones in the direction of the first line of osteocyts (makroobj. No. IV.).

fig. B. (c.) 2. II. RE. Isolovaná retikuloendothelie s řasinkami po impregnaci $AgNO_3$ v kostní lamele. Isolated reticuloendothelial cell with the teeth-like brushes in the bone lamella. (Silver-impregnationed).

fig. B. (c.) 3. II. RE. Isolovaná retikuloendothelie s hojnými řasinkami se zanořuje ku první řadě osteocytů. Isolated reticuloendothelial cell immering towards the first line of osteocyts.

fig. B. (c.) 4. II. RE. Retikuloendothelie s řasinkovým lemem tvoří jednovrstevnou stěnu kostní kapiláry. Reticuloendothelial-brushes cells, on the basal part of arteriol's wall (macroobj. No. IV.).

fig. B. (c.) 5. II. RE. Isolovaná retikuloendothelie s přeměnou řasinek v ostré výběžky osteoblastů, kterými se zanořují ku první řadě osteocytů.
Isolated reticuloendothelial cell change of the brushes to bristled dendritical osteoblast. (macroobj. No. IV.).

fig. B. (c.) 6. II. RE. Kostní kapilára s řasinkovými retikuloendotheliemi, ze kterých pochází předchozí buňka.
Bone capillary with the brush-like reticuloendothelial cell in which is the origin of the preceiding cell. (macroobj. No. IV.).

fig. B. (c.) 7. II. RE. Reticuloendothelie s řásinkovým lemem obráceným ku osteocytu prvního řádu (po impregnaci $AgNO_3$).
Reticuloendothelial with brush-like cells turned towards osteocyt of first line (macroobj. No. IV.). (silver-impregnated).

fig. B. (c.) 8. II. RE. Argentaffinní retikuloendothelie s kartáčkovým lemem přijímá a hromadí v cytoplasmě hrubozrnnou Fe. hmotu z hommogenní kostní hmoty a přetváří se zvolna v osteoblast.
Brush edged reticuloendothelial argentaffine cell accepts Fe from the homogenious bone substance and changes slowly in osteoblast. (makroobj. No. IV.).

TABUL. No. XVI.

fig. B. (c.) 1. II. RE. Argentaffinní plášť retikuloendotheliální subperiostální na trámci houbovité kosti (po impregnaci Ag). Část kosti, kde není tato argentaffinní mřížka, se neimpregnuje.
Argentaffine cover reticuloendothelial subperiostal, on the spongious bone (silver-impregnated and black). Without the cover the bone is white and nonargentaffinne (macroobj. No. IV.).

fig. B. (e.) 2. II. RE. Velké retikuloendothelie na stěnách kostních nutritivních arteriol
Large reticuloendothelial cells on the walls of nutritive arteries (macroobj. No. IV.).

fig. B. (e.) 3. II. RE. Deskriptivní průmět Haversova systému s centrál. arteriolou a s řasinkami retikuloendothelií.
Descriptive projection Haversian's arteriole. Retikuloendotheliale brush edged cells on the wall of arteriole (makroobj. No. IV.).

fig. B. (e.) 4. II. RE. Dvě velké retikuloendothelie s řasinkami v lakůnách kostní tkáně impregnované Fe hrudkovitým pigmentem se přetvořují v osteoblasty.
Two reticuloendothelial cells with brushes in lacunes of bone substance impregnated with Fe pigment changing in osteoblast. (macroobj. No. IV.).

fig. B. (e.) 5. II. RE. Transversální zlom trámcem houbovité kosti s příčnými odlomy Haverských kanálků.
Haverse's system transversal fracturated with nutritives channels (macroobj. No. IV.—bone No. 4).

fig. B. (c.) 6. II. RE. Povrchní řady osteocytů s jemnými plasmatickými výběžky.
Dendritical mesh-work of osteocyt's (macroobj. No. IV.).

TABUL. No. XVII.

fig. B. (c.) 7. II. RE. a.) b.) Argentafinní endotheloretikulární buňka z plochy s malým jádrem odloupnutá z argentaffinního pláště endostálního.
Reticuloendothelial cell, argentaffine-surface, small nucleus separated from endostale argentaffinne wire-work (filter-like) a. (overexponate), b. (underexponated).

fig. B. (c.) 8. II. RE. Argentaffinní endotheloretikulární buňka z plochy (podexponováno).
Reticuloendothelial, argentaffine cell direct view (underexponated).

fig. B. (c.) 9. II. RE. Velká retikuloendotheliální buňka interkalární části lymfatického systému má funkci uzávěrové chlopně (buňka Petrbokova, macroobj. No. IV.).
Large reticuloendothelial cell from intercalar part of lymfatic system, fundionelly valvule-like (cell of Petrbok).

fig. B. (c.) 10. II. RE. Konická retikuloendothelie (buňka Petrbokova) na odstupu krevních kapilár v kapiláry lymfatické.
Large and big pyramidal cell (Petrbok's cell) between blood and lymphatic capillary systems.

fig. B. (c.) 11. II. RE. Svit cytoplasmy v dopadajícím světle v buňce Petrbokově.
Luminiscency of cytoplasma reticuloendothelial, valvule like Petrbok's cell (fotoexposition 3 minutes) in oblique light.

fig. B. (c.) 12. II. RE. Velká (makroendothelie) Petrbokova v kapilárním lymfatickém oblouku. V procházejícím světle je tmavá, pohlcuje světlo.
Large, closed Petrbok's cell in arch of lymf capillary nonluminiscenting in transverse light (macroobj. No. IV.).

TABUL. No. XVIII.

fig. B. (c.) 14. II. RE. Argentaffinní, retikuloendotheliální mřížka tvoří samostatný válcovitý plášť na trámci houbovité kosti. Velká retikuloendothelie na protilehlém kostěném valu má knoflíkovitě prominující jádro (po impregnaci $AgNO_3$).
Reticuloendothelial, argentaffine wire-works forms an cylindrical solitary cover. The big reticuloendothelial on the opposite side of the bone wall has a big button-like nucleus (silver-impregnation) (macroobj. No. IV.).

fig. B. (c.) 15. II. RE. Krevní splav v houbovité kosti s vývojovými řadami buněk (RES) retikuloendotheliálního systému obsahujícím Fe figment. Fibrinoretikulární síť tvoří ve splavu odvodnou kapiláru.
Blood sinuses and the haemoglobinogenic different types of reticuloendothelial cells infiltrated Fe pigment in spongious bones (macroobj. No. IV.).

fig. B. (c.) 16. II. RE. Po délce obnažený krevní sinus s různými vývojovými stadii retikuloendothelocytů-haemoglobinogenních.
The different genetio stadium of reticuloendothelial haemoglobinogenetic cells sinus along, (macroobj. No. IV—bone No. 1).

fig. B. (c.) 17. II. RE. Fibrinoretikulární kapilára, ve které dozrávají retikuloendothelie haemoglobinogenní a odkud se podobnými kapilárami nasávají do extramedulárního cirkulačního systému krevního.
Fibrinoreticulare capillary in which reticuloendothelial cells are ripening and from where they are exhausted into the extramedulare circulation system. (macroobj. No. IV.).

fig. B. (c.) 18. II. RE. Pohled do sinusu, ve kterém dozrávají erythroblasty opatřené velkým puchýřovitým jádrem.
Large, ripening erythroblast with ball-like nuclei in the blood sinus (macroobj. No. IV.—bone No. 1).

TABUL. No. XIX.

fig. B. (c.) 19. II. RE. Dva erythroblasty vypuzují jádro do lymfatických kapilár.
Two erythroblasts expulsing nucleus into lymphatic capillary (macroobj. No. IV.—bone No. 1).

fig. B. (c.) 20. II. RE. Hroznovité útvary dozrávajících erythroblastů v krevním sinusu s velikými puchýřovitými jádry.
Grape-like ripining erythroblasts in sinuses of blood (macroobj. No. IV.—bone No. 1).

fig. B. (c.) 21. II. RE. Vývojová řada granulocytů z kostní dřeně cylindrické kosti.
Genetic line of macrogranulocytes from the marrow of cylindrical bone (macroobj. No. IV.—bone No. 1).

fig. B. (c.) 22. II. RE. Isolovaný erythroblast s velkým okrouhlým plasticky modelovaným jádrem je neprůsvitný.
Isolated erythroblast, with ball-like nucleus non transparent from blood sinuses marrow (macroobj. No. IV.—bone No. 1).

fig. B. (c.) 23. II. RE. Nahloučené endotheloretikulární buňky z lymfatické kapiláry jsou argentaffinní.
Accumulated endotheloreticulares cells of lymph capillare are, argentaffinnes (macroobj. No. IV.—bone No. 1).

fig. B. (c.) 24. II. RE. Nahloučené endotheloretikulární buňky z lymfatické kapiláry v šikmém zástinu svítí (exponováno 3 minuty).
Accumulated endotheloreticulares cells of lymph capillare luminiscent in oblique light, microscopicale technique (macroobj. No. IV.—bone No. 1).

fig. B. (c.) 25. II. RE. Vyzrálý makrofág-granulocyt ze dřeně cylindrické kosti.
Ripe macro-granulocyt of the marrow of cylindrical bone (macroobj. No. IV.—bone No. 3).

TABUL. No. XX.

fig. B. (d.) 1. II. Lymfatická kapilára s interkalární (vsunutou) částí přehrazenou mokroendothelií Petrbokovou.
Lymphatic capillary intercalare part divided by large macroendothelial Petrbok's cell.

fig. B. (d.) 2. II. Stejný úsek kapiláry svítí v napadajícím šikmém světelném zástinu.
Luminiscented lympha in oblique light, histological microtechnique (macroobj. No. IV.—bone No. 1).

fig. B. (d.) 3. II. Systémy lymfatických váčků spojených průsvitnými lymfatickými kapilárami s neprůsvitnou kapilárou a krevním vakem v dol. části obrazu.
Lymphatic and blood sacs united with capillaries of blood system (black) and lymphatic system (white) (macroobj. No. IV.).

fig. B. (d.) 4. II. Vakovité lymfatické kostní dutiny voskově matné při světle procházejícím.
Lymphatic sacs in transversale light are wax-like.

fig. B. (d.) 5. II. Tytéž lymfatické vaky při světle šikmého zástinu svítí.
Lymphatic sacs in oblique light luminiscent (macroobj. No. IV.—bone No. 1).

TABUL. No. XXI.

fig. B. (d.) 6. II. Svítící interkalární (vsunutá) část lymfatické kapiláry a v ní černá, laločnatá hmota jádra uzávěrové makroendothelie Petrbokovy.
Luminiscenting lymphatic mass shows lobeted nucleus of Petrbok's macroendothelial cell.

fig. B. (d.) 7. II. Větvení lymfatické cévy s voskově matným vzhledem.
Ramificated lymphatic capillary (wax-like view).

fig. B. (d.) 8. II. Svítící cytoplasma retikuloendothelií lymfatických cév.
Luminiscenting cytoplasma of reticuloendothelial lymphaticales cells in oblique light, michoscopicale technique.

fig. B. (d.) 9. II. Větvení lymfatickéí cévy lymphoepitheloidními buňkami.
Ramificated lymphatic capillary wax-like view with lymphoepitheloid cells (macroobj. No. IV.—bone No. 1).

fig. B. (d.) 10. II. Úlomek dřeně kostní s různými vývojovými stadii macrogranulocytů a buněk řady lipofágů.
Fragment of bone marrow with different genetical stadiums of granulocytes (karyokinesis middle part of picture).

fig. B. (d.) 11. II. Lymfatické vaky podobné šípkům se sběrnými vlnovitě zprohýbanými kapilárami.
Lymphatic sacs similar to the fruit of the dog-rose with undulated lymphatic fissures (macroobj. No. IV.—bone No. 1).

TABUL. No. XXII.

fig. B. (d.) 12. II. Pohled shora na vlnovitě zprohýbané lymfatické štěrbiny, které se zanořují do hloubky a navzájem tvoří husté svazky jemných štěrbin.
Uudulated lymphatic capillary going into depth and forming together thick fascicles of fissures. (View from abov.)

fig. B. (d.) 13. II. Soubor jemných štěrbin v základní kostní hmotě, tvoří štětcovité útvary vložené mezi konce krevních kapilár a začátek lymfatických cév.
Fascicles of fines fissures in bone substance form penicillious-like microobjects situated between the ends of blood capillaries and beginning of lymphatic vessels (macroobject No. IV.—bone No. 3).

fig. B. (d.) 14. II. Dvě paralelní kapiláry končí v systémech lymfatických štětcovitých fissur. Mezi oběma je distinktní hranice. Levá céva patří krevnímu kapilárnímu úseku a pravá céva je vsunutá část lymfatického filtračního úseku.
Two parallel capillaries (blood and lymph) end in lymphatical pennicillious-like fissures of haemolymph and of lymph, where haemolymph changes to lymph.

fig. B. (d.) 15. II. a, b. Příčný zlom prstencovitým kostním pláštěm filtračního systému plasma-haemolymfa-lymfa. Krevní kapiláry v šikmém zástinu nesvítí (hoření část kostěného prstence obsahuje dvě arterioly), kdežto zkondensovaná haemolymfa uprostřed lymfatické cévy jasně svítí i s odstupujícími lymfatickými cévami dole vlevo.

fig. B. (d.) 15. II b, a Transversale fracture of lymphatic filtration's microsystem, where upper blood capillaries are untransparent and black, haemolymph luminiscent rose transformes into lymph (white luminiscent).

TABUL. No. XXIII.

fig. B. (d.) 16. II. Větvení lymfatických cév užší vpravo má velkou Petrbokovu buňku v interkalární lymfatické části.
Ramificated lymphatic vessels with macroendotheliale cell of Petrbok intercalare part's of lymphatic capillaries.

fig. B. (d.) 17. II. Voskově matná lymfa v cévách při šikmém zástinu svítí.
The same ramificated lymphatic vessels in oblique light luminiscente. Nuclei of endothelia, and of lymphoepithelia are pitch-black.

fig. B. (d.) 18. II. Větvení lymfatických cév v houbovité kosti (v procházejícím světle).
Large ramificated lymphatic vessels in spongious bone in transversal light are black.

fig. B. (d.) 19. II. Tytéž lymfatické cévy svítí v šikmém osvětlení. Jádra endotheliálních presorických buněk Petrbokových jsou laločnatá, smolně černá.
The same big ramificated lymphatic vessels in spongious bone in oblique light (luminiscentes). Nuclei of endothelial pressures Petrbook's cells are lobet and pitch-black.

TABUL. No. XXIV.

fig. B. (d.) 20. II. a. Na kmeni arterie je pupenovitý matný váček, do něhož se zanořují krevní kapilární systémy. Ve váčku se osmosou tvoří haemolymfa a lymfatickými kapilárami se odvádí do lymfatického systému.
a) On the arterial wall lymphatic sacs containing haemolympha from blood capillaries filtred to lymphatic capillaries (in transversal light forms Röntgen-like negative).

fig. B. (d.) 21. II. b. Haemolymfatický váček naplněný svítící haemolymfou (v šikvém zástinu).
b) On the arterial wall there is a lymphatic microfiltration sac, where lymph is separated from blood to lymphatic capillaries (in oblique light luminiscent Röngen-like positive).

fig. B. (d.) 22. II. a. Haemolymfatická céva po odstupu z filtračního váčku naplněná voskově matnou lymfou.
a) After separating from lymphatic sac is the lymphatic vessel waxy-dull (röntgen-like negativ).

fig. B. (d.) 23. II. b. Po odstupu z lymfatického váčku je naplněna svítící haemolymfou.
b) The same ramificated lymphatic vessel luminiscente in oblique light (Röntgen-like positiv).

fig. B. (d.) 24. II. a. Anastomosy mezi lymfatickými váčky (v procházejícím světle).
Anastomosies between lymphatical sacs in transversal light (Röntgen-like negativ).

fig. B. (d.) 25. II. b. tytéž systémy lymfatických vaků s anastomosami svítí při šikmém osvětlení.
b) systems of lymphatical sacs and anastomosis in oblique light (luminiscentes Röntgen-like positive).

TABUL. No. XXV.

fig. B. (d.) 26. II. a. Haemolymfatický váček z houbovité kosti (v průsvitu voskově matný, opaleskuje). Arterioly se větví ve váčku a osmosou se zde tvoří různě koncentrovaná haemolymfa (růžová), až lymfa bíle v zástinu svítící.
Haemolymphaticale sac with blood capillaries and with lymph capillaries in spongious bone (transversale light, preduces Röntgen-like negative).

fig. B. (d.) 27. II. b. Haemolymfatický váček s krevními a lymfatickými kapilárami v šikmém zástinu bíle svítí. Tmavá jádra makroendothelií Petrbokových (pressorických).
Luminiscency of haemolymphatic sac (Röntgen-like positive picture). The large nuclei of Petrbok's pressure cells are pitch-black, nuclei lymphoepitheliale cells are wax pitch-black (macroobj. No. IV.—bone No. 1).

fig. B. (d.) 28. II. a. Silná přívodní orteriola vúsťující do haemolymfatického váčku. Velká pressorická buňka uzavírá ústí arterioly (při procházejícím světle).
The large blood arteria is situated above on the left side of lymphatic sac. At end of blood arteria flowing into the lymphatic sac are makroendothelia called Petrbok's closing cells.

fig. B. (d.) 29. II. b. Svítící lymfa v lymfatických cévách s temnými laločnatými jádry makroendothelií Petrbokových.
Luminiscenting lymph in lymphatic sac and lymphatic capillaries with large lobet nuclei of macroendotheliale Petrbok's cells.

TABUL. No. XXVI.

fig. B. (d.) 30. II. a. Haemolymfatický váček z houbovité kosti. Arterioly se větví uvnitř a transudací se zde tvoří různě koncentrovaná haemolymfa (v procházejícím světle — tmavá).
Hoemolyphatic sac of spongious bone. After transudation of the haemolymph to lymph the concentrated lymph flows to lymph vessels (transversal light make Röntgen-like, negative picture).

fig. B. (d.) 31. II. b. Haemolymfatický váček v šikmém zástinu svítí.
Intensive lightening haemolymphatical sac gives in oblique light a Röntgen-like positive picture (macroobject No. IV,—bone No. 1).

fig. B. (d.) 32. II. a. Odlomená lymfatická céva s makroendotheliemi v procházejícím světle je voskově matná.
Fracutred lymphatical vessel with macroendothelial cells in transversal light (röntgen-like negative picture).

fig. B. (d.) 33. II. b. Odlomená lymfatická kapilára s makroendotheliemi v šikmém zástinu svítí.
Fracturated lymphatic vessel with macroendothelial cells in oblique light make röntgen-positive picture.

fig. B. (d.) 34. II. a. Lymfatický vak v procházejícím světle s laločnatým jádrem Petrbokovy makroendothelie (voskově temný).
Large lymphatical sac in transversal light with lobet nucleus of macroendothelial cell-Petrbok's (Röntgen-like negative picture).

fig. B. (d.) 35. II. b. Lymfatický vak v šikmém zástinu uvnitř svítí méně a na zevní části intensívně. Laločnaté jádro makroendothelie je podoby karyokinetického vřeténka se světlejšími a tmavšími stíny pentlic.
Intensive-luminiscency in haemolymphatical sac. Large lobeted nuclei of macroendothelial cell. Karyokinesis-like figure of Petrbok's large cell (röntgen-like positive picture macroobj. No. IV.—bone No. 1).

TABUL. No. XXVII.

fig. B. (d.) 36. II. Odlomená část lymfatického váčku v šikmém zástinu bíle svítí.
Fractured part of lymphatic sac in oblique light (röntgen-like positive picture).

fig. B. (d.) 37. II. Část vývodního lymfatického systému s makroendothelií Petrbokovou, která má tmavé laločnaté jádro s naznačenou karyokinesou. V šikmém zástinu lymfa svítí a jádra lymfoepithelií jsou tmavě šedá a pohlcují světlo.
Luminiscency of lymphatic sac with large, lobed Petrbok's macroendothelial cell (nuclear karyokinesis).

fig. B. (d.) 38. II. Lymfatická céva se svítící lymfou a tmavými laločnatými jádry v šikmém zástinu.
Luminiscency of lymphatic vessels with lobet giant endothelial cells-nuclei (in oblique light, Röntgen-like positive picture, macroobj. No. IV.—bone No. 1).

fig. B. (d.) 39. II. Lymfatická céva v procházejícím světle je voskově matná petrifikovanou lymfou.
Lymphatic vessel in transverse light (Röntgen-like negative-picture), shaded in the middle part by superposed calcit lamella.

fig. B. (d.) 40. II. Lymfatická céva v šikmém zástinu svítí. Céva je napříč zastíněná lamelami kalcitu, který je pro šikmé světlo neprostupný a pohlcuje svit petrifikované lymfy.
Luminscency of petrificated lymph-vessel cemented in calcit lamella unpenetrable for oblique light (macroobj. No. IV.—bone No. 1).

fig. B. (d.) 41. II. Laločnaté jádro makroendothelie Petrbokovy, která má presorickou funkci chlopně a reguluje směr toku lymfy v rozvětvujících se kapilárních obloucích interkalárního systému.
Large lobet macronucleus in walvule-like and pressorique Petrbok's cell ... above cross-road of intercalare capillaries, of lymphatic system (macroobj. No. IV.—bone No 1).

fig. B. (d.) 42. II. Intensívní svit (v šikmém zástinu) cytoplasmy makroendothelie Petrbokovy ve stadiu dvou separovaných jader po ukončené karyokinesi
Intensive luminiscency of the pressorique, valve-like, Petrbok's cells. Stadium after karyokinesis—two separated nuclei and cells (macroobj. No. IV.—bone No. 1).

TABUL. No. XXVIII.

fig. C. (a.) 1. II. Mikroskopická plsť z fibrocytů a leiomyocitů, které tvoří perivaskulární část stěn velkých tepen.
Mesh-work composed from leiomyocyts, fibrocyts in the wall of big artery (macroobj. No. IV.—muscles).

fig. C. (a.) 2. II. Příčně pruhované kosterní svalstvo s fibrocyty intersticia. Podélné a příčné pruhování patří oběma buněčným složkám.
Microscopitale structure of striped skeleton muscles and fibrocyts. Longitudinal and transversal stripping belongs to fibrocyts as well as to skeleton muscles.

fig. C. (a.) 3. II. Isolované a petrifikované vlákno kosterního příčně pruhovaného svalu. Na obvodě svalového vlákna jsou přiloženy štíhlé vřetenité fibrocyty s jádry. Uvnitř svalového vlákna jsou jádra svalové buňky.
Isolated stripped fibre of skeleton muscle (macroobj. No. IV.—bone No. 1., muscle No. 3).

fig. C. (a.) 4. II. Destička petrifikovaných svalových vláken s vidličnatě větvenou arteriolou (helicin. typu) na přechodu z periostu (okostice) do svalu. Isotropní a anisotropní hmota svalu je zachována. Podélné kontraktilní fibrily jsou dobře patrny i s temnými jádry svalových vláken.
Skeleton muscles transversally stripped with helicin. arter. between tendon, muscles and fascias. Nuclei of muscles fibrills are obscure black and contractil fibres are longitudinally stripped (macroobj. No. IV., muscles No. 3).

TABUL. No. XXIX.

fig. C. (a.) 5. II. Krystaly kalcitu s inkludovanými buňkami. Dvojlom světla v krystalických oblouclch.
Cells coming from bursae mucosae cemented in calcit crystals. Light polarisation in calcit-crystals deformitations (macroobj. No IV.—bursa mucosa No. 1).

fig. C. (a.) 6. II. Inkluse buněk bursae mucosae v krystalech kalcitu.
Cells from wall of bursae mucosae cemented in calcit-crystals (macroobj. No. IV.—bursa mucosa No. 1).

fig. C. (a.) 7. II. Přelomený krystal dvojlomého kalcitu.
Double light refracting (island-like) calcit crystal (fracturated) (macroobject. No. IV.—bursa mucosa No. 1).

fig. C. (a.) 8. II. Ohybové deformace pynakoidů a rhomboedrů ve druhé nosné vrstvě kalcitových krystalů, tvořících stěny mukosních váčků kolem kloubů.
Deformations of calcit crystal's from the wall of bursae mucosae periarticularies (macroobj. No. IV.—bursa mucosa No. 1).

fig. C. (a.) 9. II. Řady buněk upevněných na centrální krystalické mřížce, která vznikla ze zbytků myxofibromatosního vaziva.
Cell stripes fixed in wire-work of myxofibromatous ligaments cemented in calcit (macroobj. No. IV.—burs. mucos. No. 1).

fig. C. (a.) 10. II. Tmavý okraj vnitřní plochy bursae mucosae s hojnými vrstvami smolově černých neprůsvitných jader myxofibromatosních endothelií.
Black interior (of bursae mucrosae) with copious layers of endothelial cells.

fig. C. (a.) 11. II. a. b. Inkluse křídlovitých polymorfních myxofibromatosních buněk v krystalech kalcitu.
Polymorphocellulars myxofibrocyts cemented in crystals of the wall bursae mucosae (macroobj. No. IV.—burs. mucos. No. 1).

TABUL. No. XXX.

fig. C. (a.) 12. II. Mnohočetné křídlovité, polymorfní buňky a jádra myxofibromatosního vaziva z mukosních váčků (burs. mucos) v prismatech a deskách dvojlomného kalcitu.
Winged myxofibromatous cells cemented in iceland-like double refracting calcit (bursae mucosae—macroobj. No. IV.).

fig. C. (a.) 13. II. Deska dvojlomného kalcitu s inklusemi křídlov. myxofibromatosních buněk tvořících guirlandovité závěsy v osách krystalisačních mřížek.
Winged myxofibromatous cells cemented in lamelle of calcit form guirlande-like figures.

fig. C. (a.) 14. II. Hojné buničné inkluse v závěsech na centrální krystalisační mřížce, jako na pavučinách přichycené.
Winged myxofibromatous cells fixed on wire-work similar to that of spider's work.

fig. C. (a.) 15. Pavučinovitá krystalisační mřížka se zbytky buněk a jader myxofibrosního vaziva ve dvojlomném kalcitu.
Shadows of myxofibromatous cells and nuclei in double refracting layers of iceland-like calcit (macroobj. No. IV.—burs. mucos. No. 1).

TABUL. No. XXXI.

Makroobjekt I. Petrifikovaný mozek velikého savce. Pohled shora. Foto J. Petrbok

TABUL. No. XXXII.

Makroobjekt II. Petrifikovaný mozek velikého savce. Pohled zdola. Foto J. Petrbok.

TABUL. No. XXXIII.

Makroobjekt III. Petrifikovaná páteř s míšním obsahem shora a zdola. Foto A. Pilát.

TABUL. No. XXXIV.

Makroobjekt IV. Petrifikované kosterní svaly s úpony na kost a otevřené dutiny mukosních váčků (Burs. mucosae). Foto A. Pilát.

SBORNÍK NÁRODNÍHO MUSEA V PRAZE - ACTA MUSEI NATIONALIS PRAGAE

XVI, 1960/B (přírodovědný), No. 3.

Redaktor:
Člen korespondent ČSAV ALBERT PILÁT, doktor biologických věd.

J. Jerman: Paleohistologické nálezy v riss-würmských travertinech z naleziště Hrádok—Gánovce u Popradu Československo). — Paleohistological, researches in Riss-Würm travertines in the area Hrádok—Gánovce near Poprad (Czechoslovakia).

V červenci 1960 vydalo svým nákladem v počtu 800 výtisků Národní museum v Praze.
Vytiskl Knihtisk 1, n. p., v Praze 1-Malá Strana, Karmelitská 6.

Cena brožovaného výtisku 8 Kčs.

A-10*01257

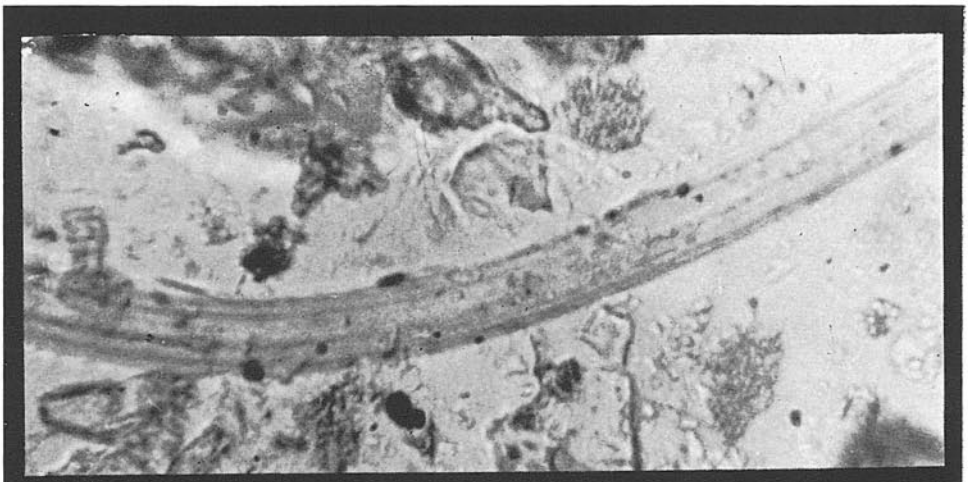

fig.1./a.//I.

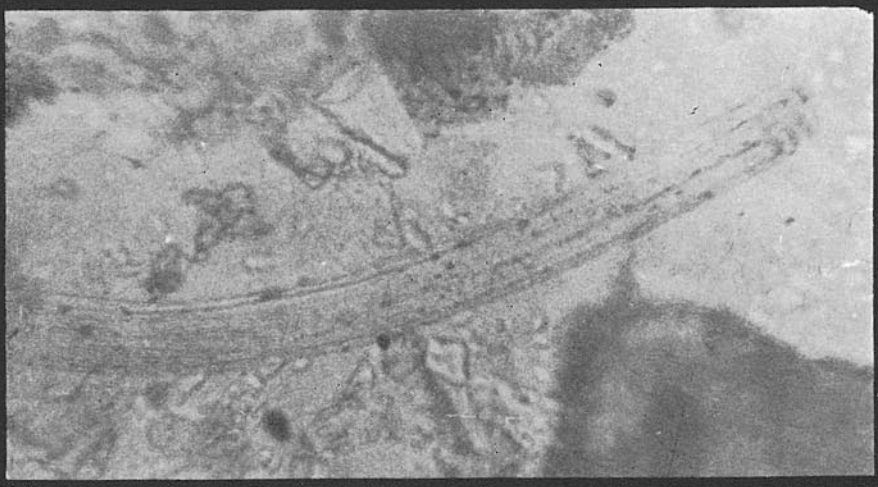

fig.1./b.//I.

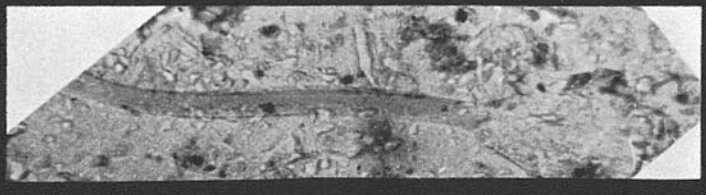

fig.1./c.// I.

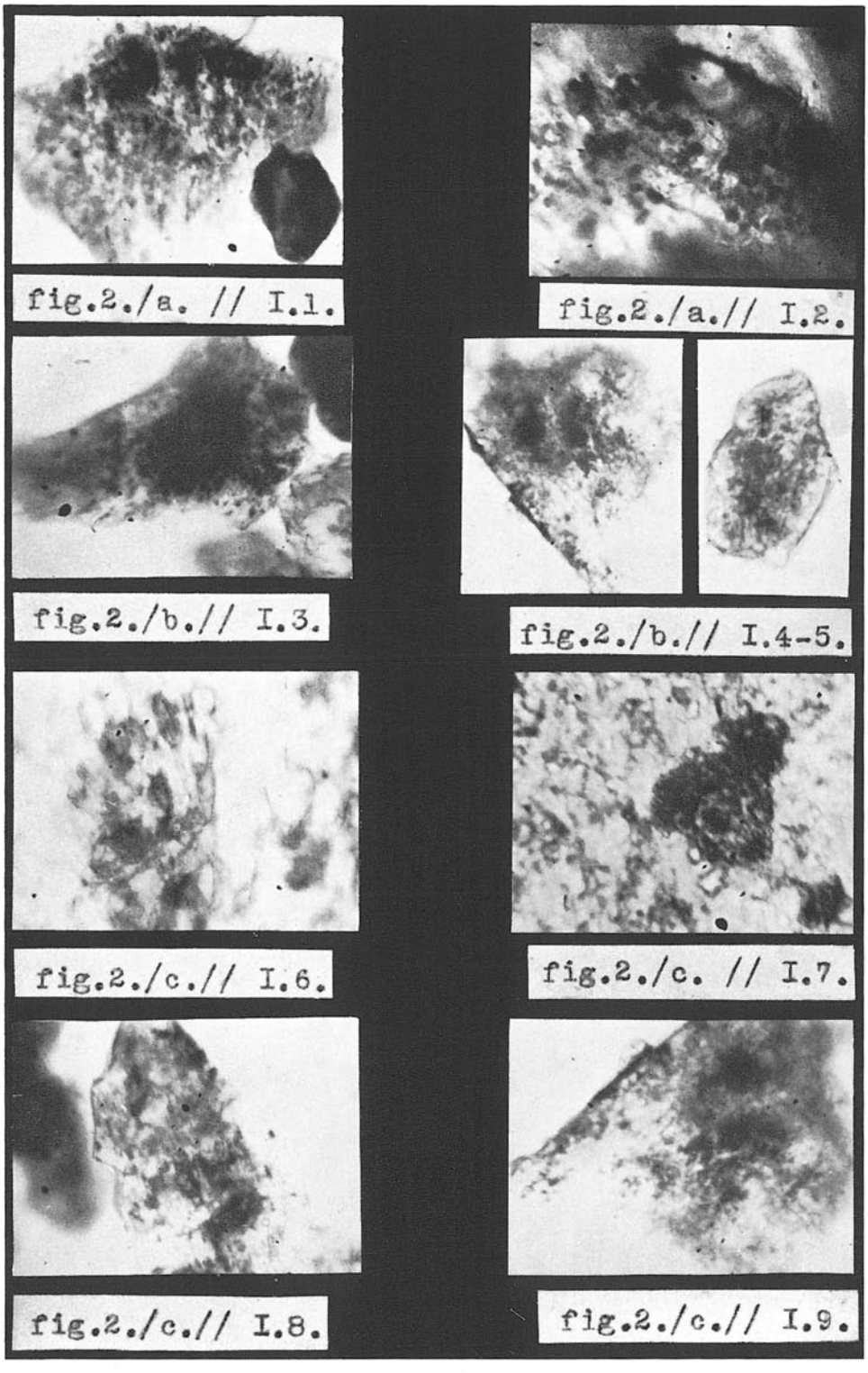

fig.2./a. // I.1.

fig.2./a.// I.2.

fig.2./b.// I.3.

fig.2./b.// I.4-5.

fig.2./c.// I.6.

fig.2./c. // I.7.

fig.2./c.// I.8.

fig.2./c.// I.9.

Fig.3./d.//I glia 1.

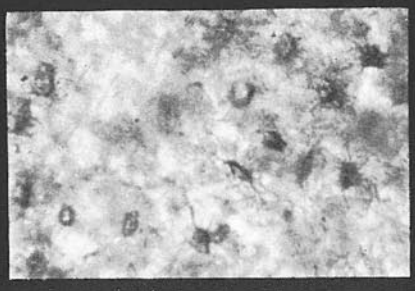

Fig.3./d.//I glia 2.

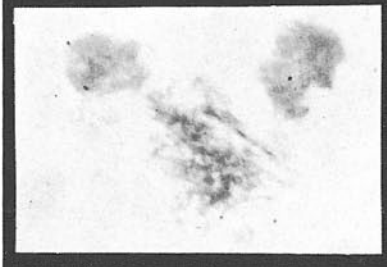

fig.3./d.// I glia 3.

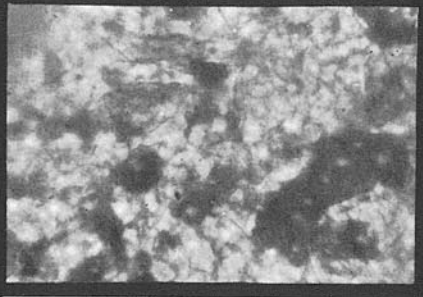

fig.3./d.// I glia 4.

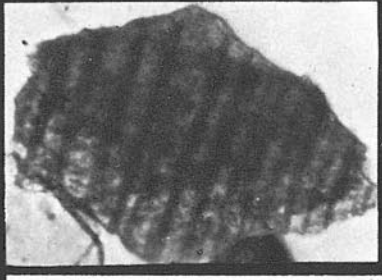

fig.3./d.// I glia 5.

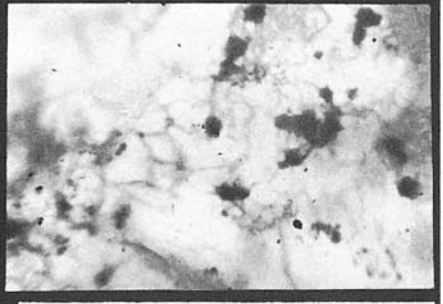

fig.3./d.// I glia 6.

fig.3./d.// I glia 7.

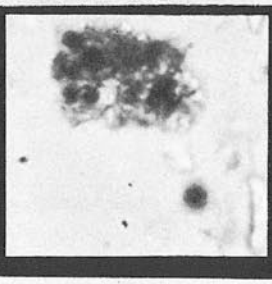

fig.3./d.// I glia 8.

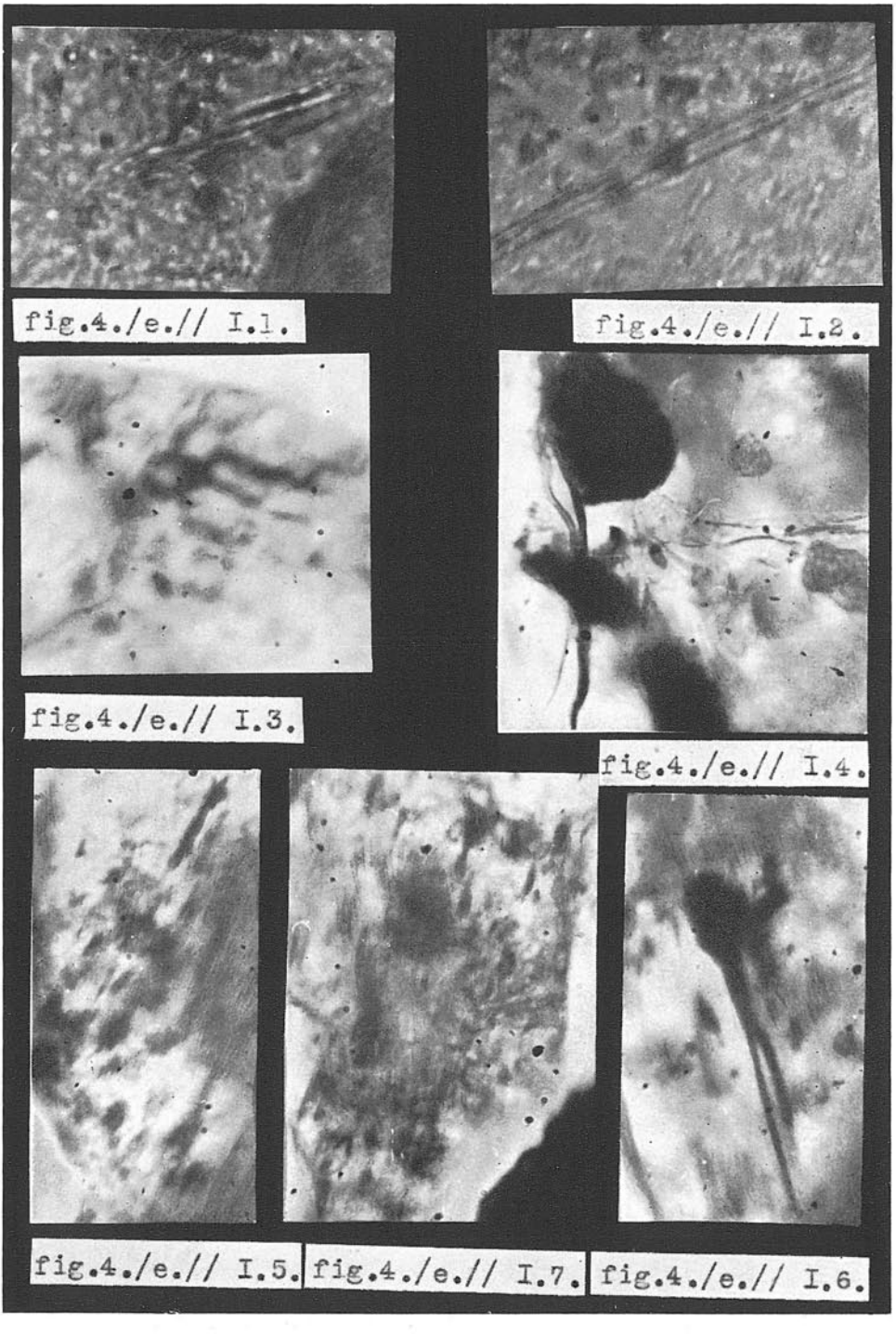

fig.4./e.// I.1.

fig.4./e.// I.2.

fig.4./e.// I.3.

fig.4./e.// I.4.

fig.4./e.// I.5.

fig.4./e.// I.7.

fig.4./e.// I.6.

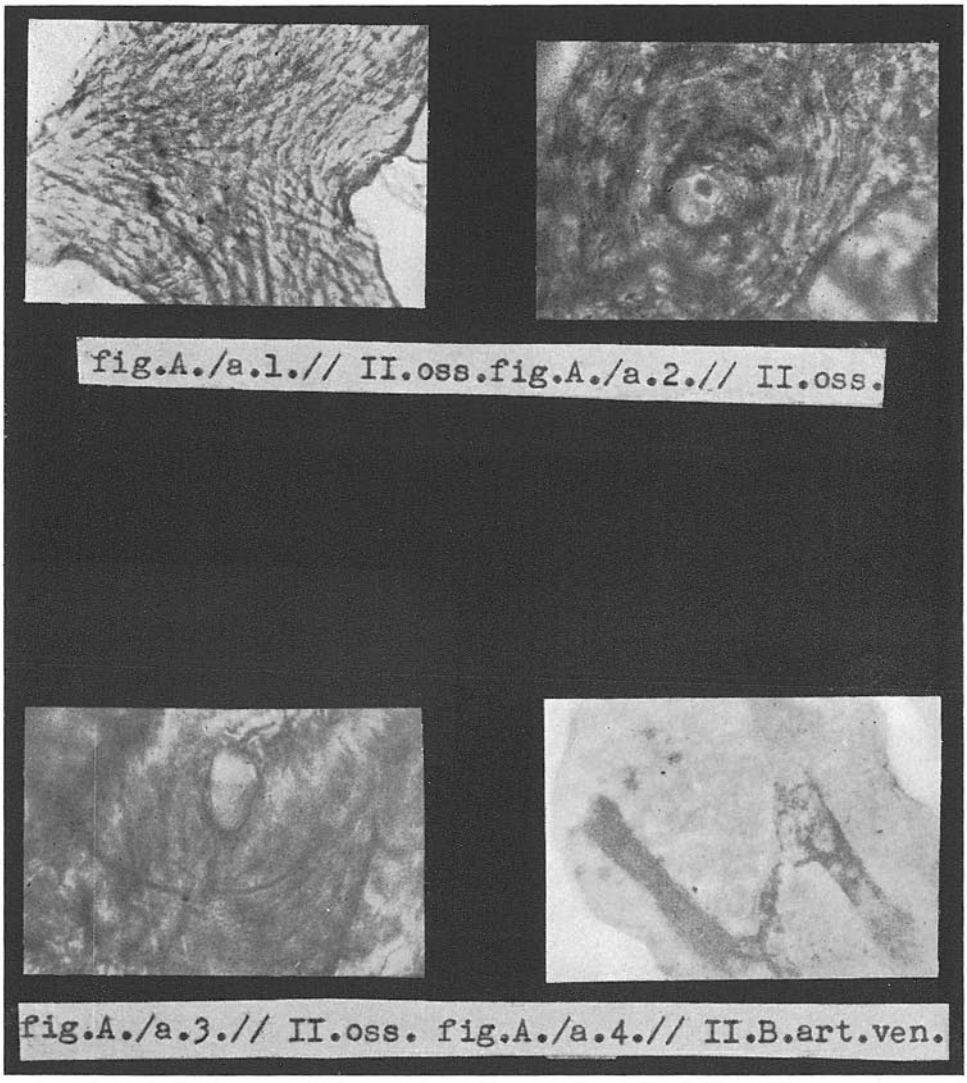

fig.A./a.1.// II.oss.fig.A./a.2.// II.oss.

fig.A./a.3.// II.oss. fig.A./a.4.// II.B.art.ven.

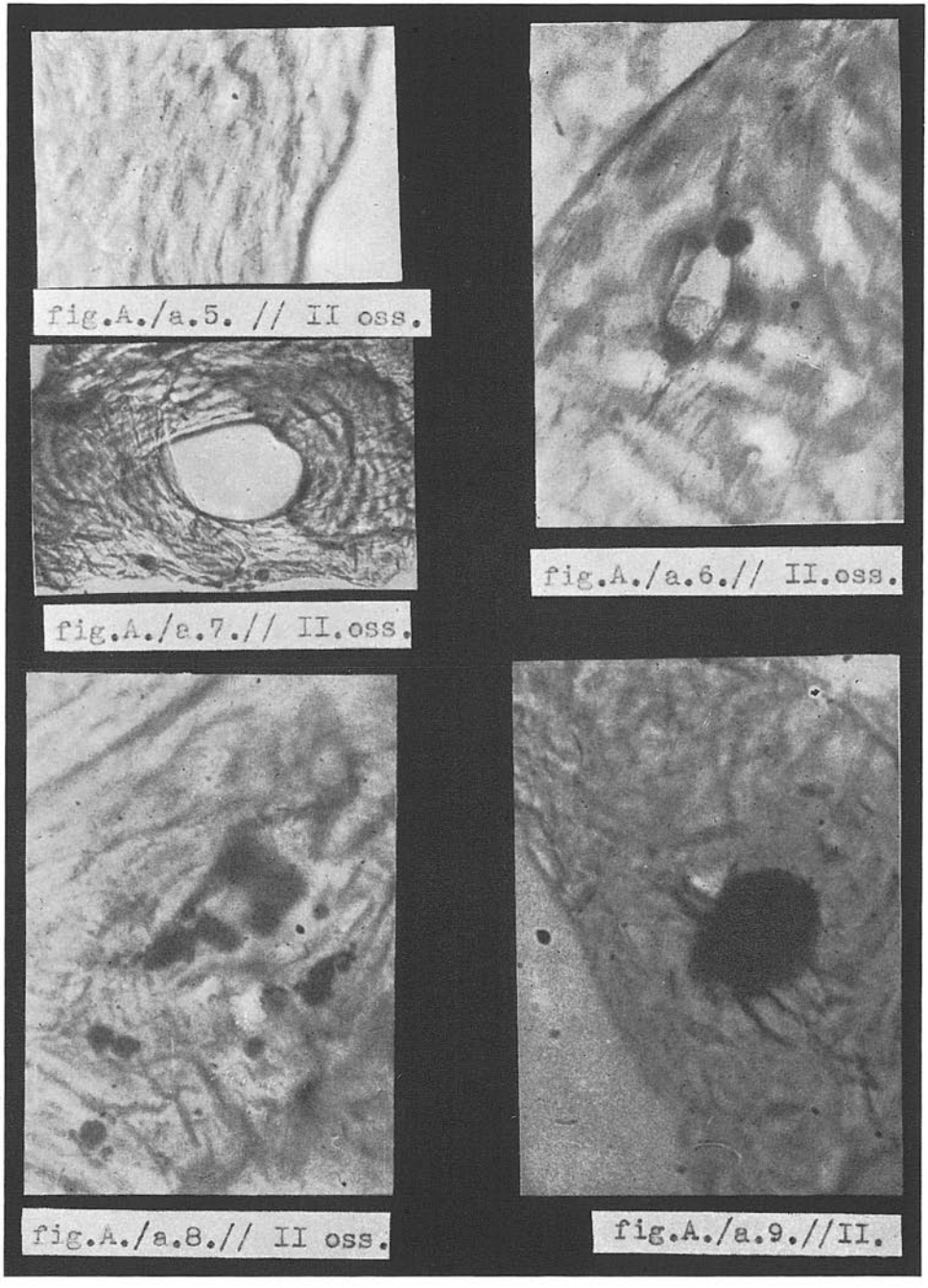

fig.A./a.5. // II oss.

fig.A./a.6.// II.oss.

fig.A./a.7.// II.oss.

fig.A./a.8.// II oss.

fig.A./a.9.//II.

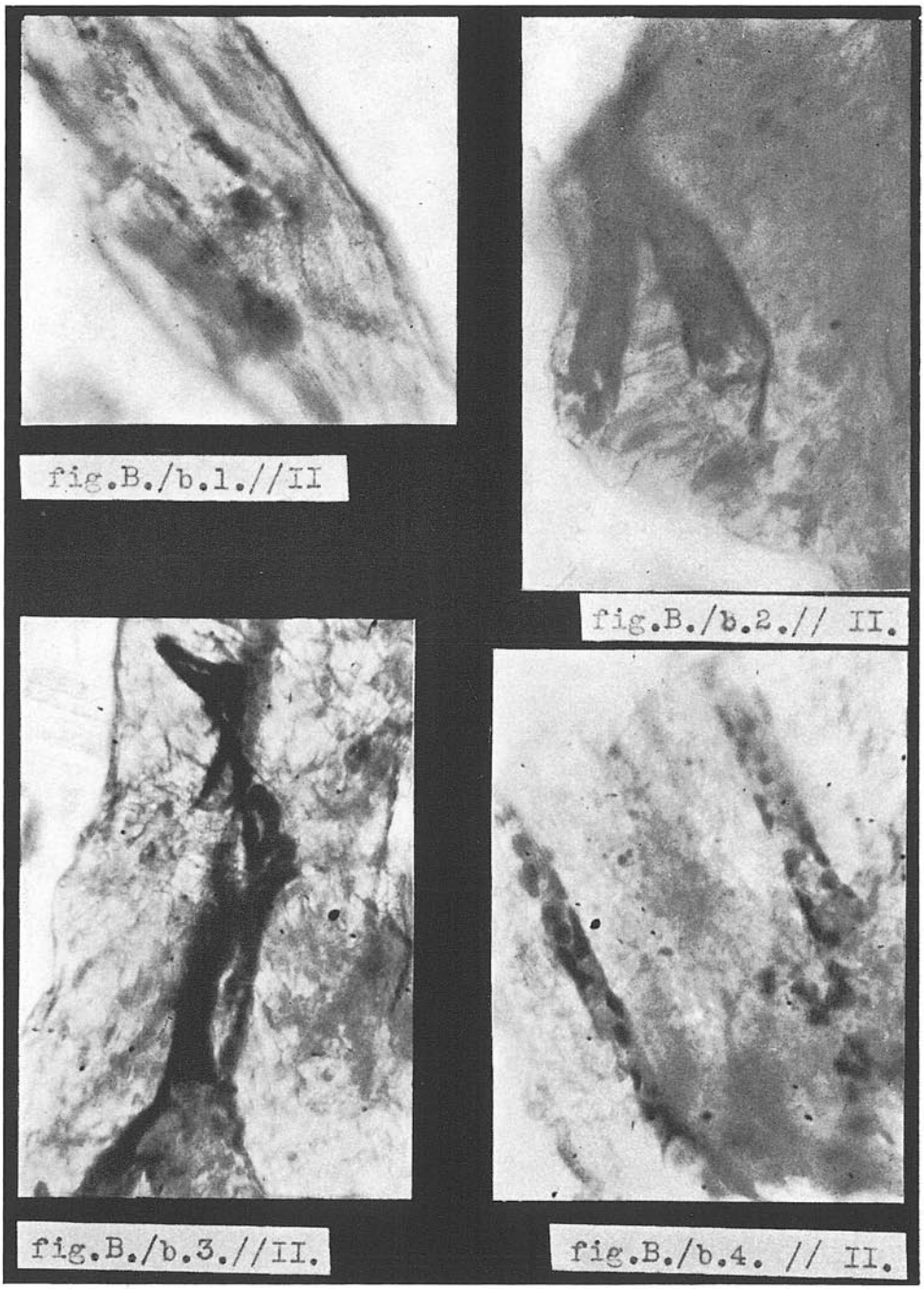
fig.B./b.1.//II
fig.B./b.2.// II.
fig.B./b.3.//II.
fig.B./b.4. // II.

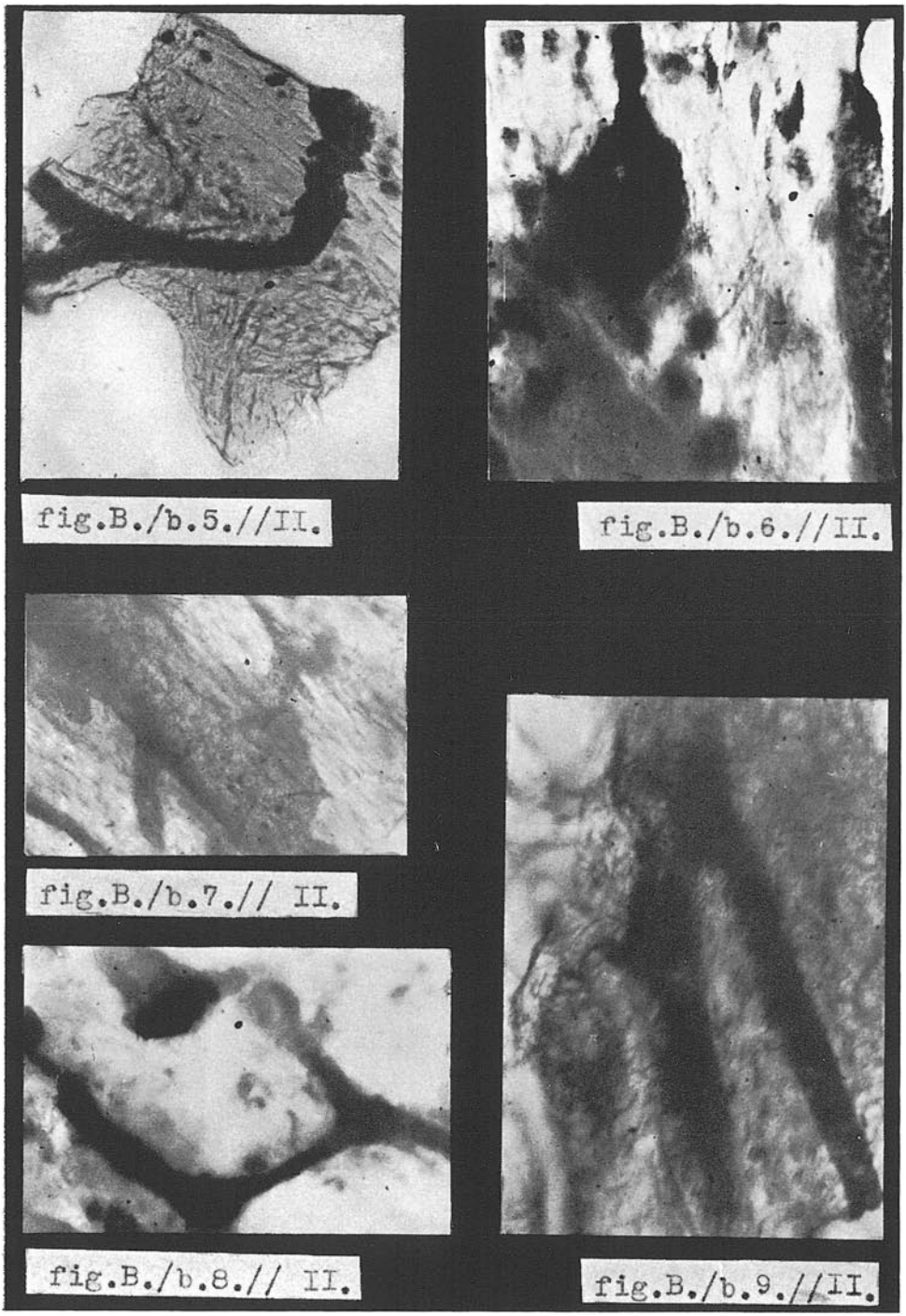

fig.B./b.5.//II.

fig.B./b.6.//II.

fig.B./b.7.// II.

fig.B./b.8.// II.

fig.B./b.9.//II.

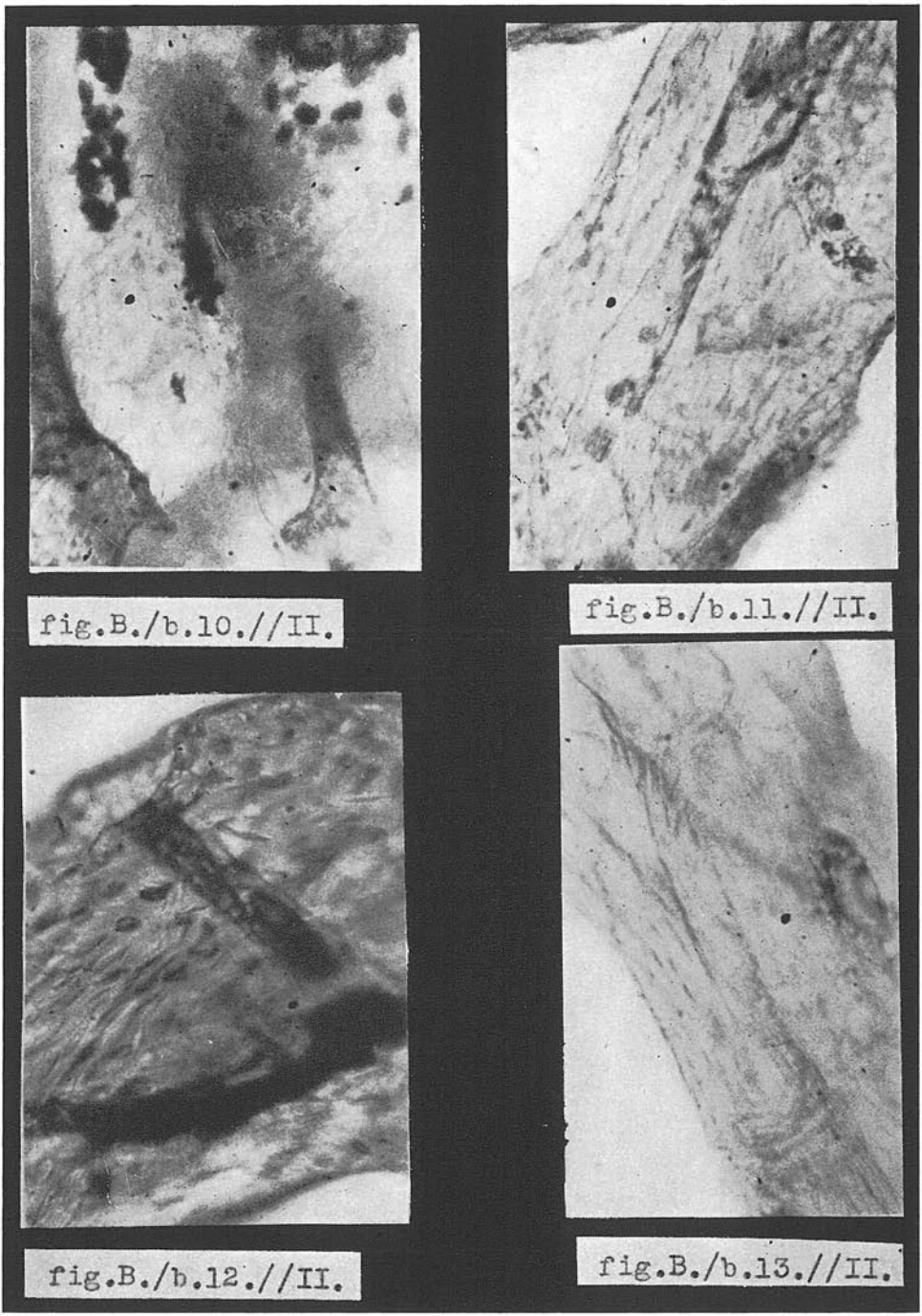

fig.B./b.10.//II.

fig.B./b.11.//II.

fig.B./b.12.//II.

fig.B./b.13.//II.

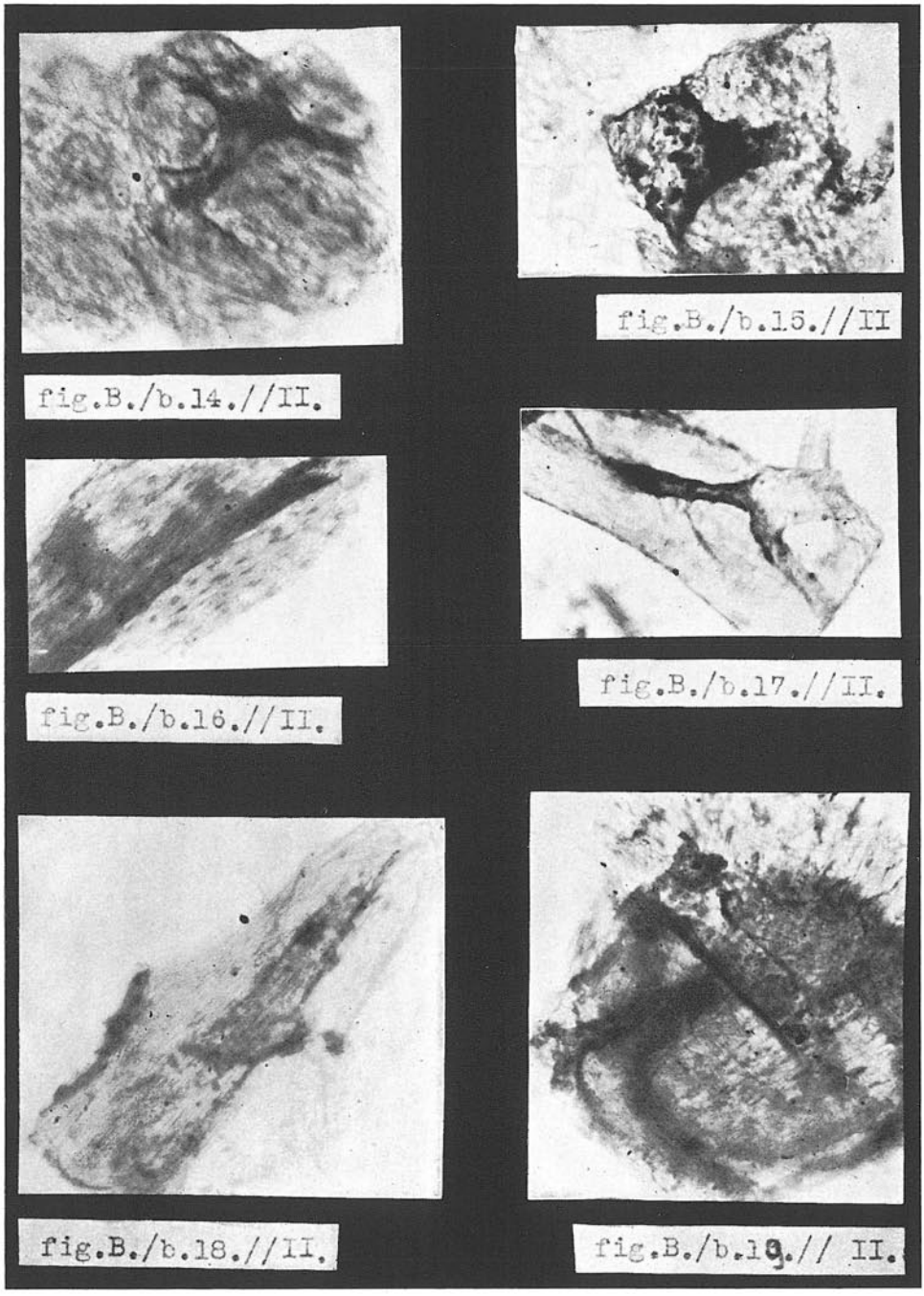

fig.B./b.14.//II.

fig.B./b.15.//II

fig.B./b.16.//II.

fig.B./b.17.//II.

fig.B./b.18.//II.

fig.B./b.19.// II.

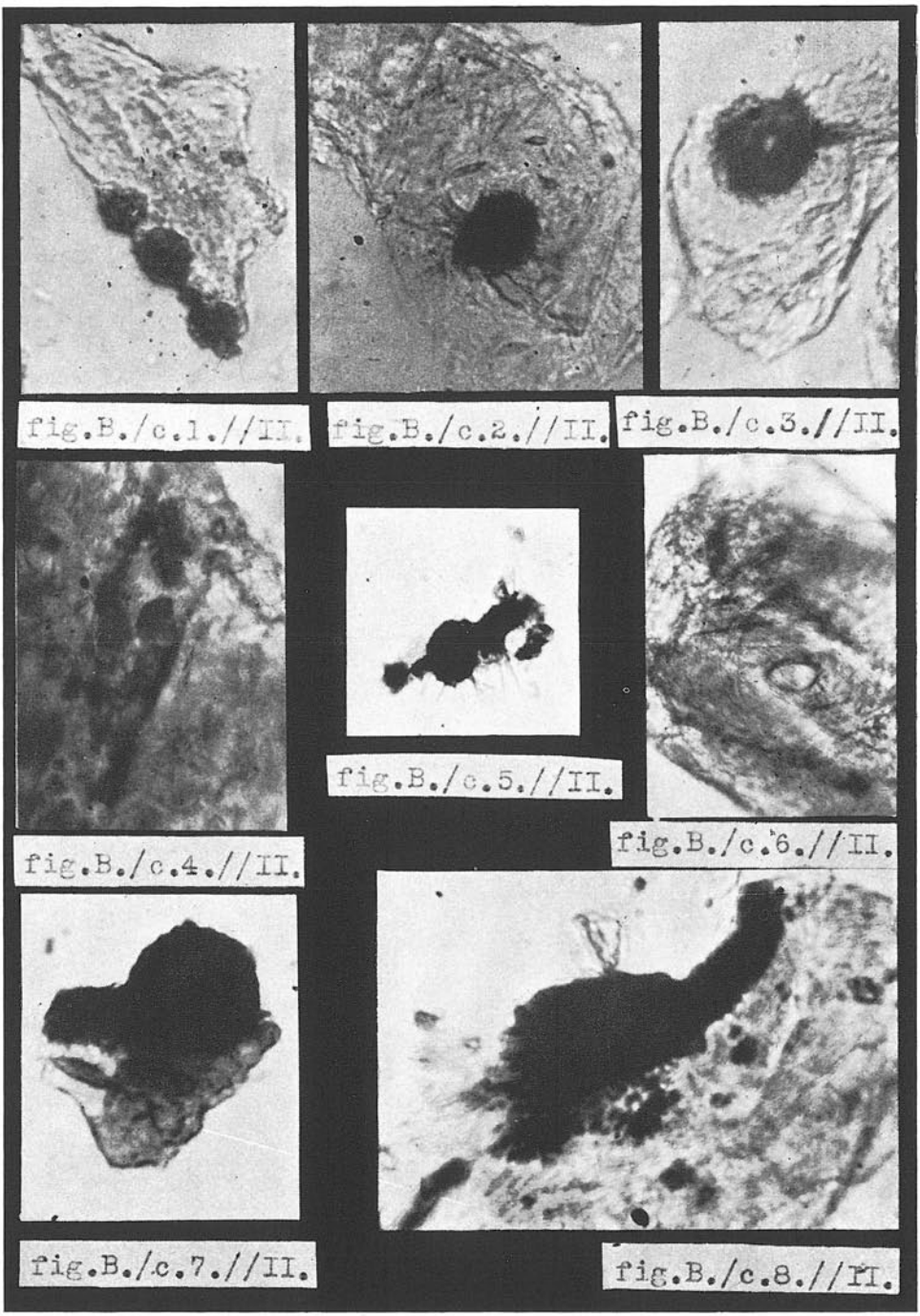

fig.B./c.1.//II.

fig.B./c.2.//II.

fig.B./c.3.//II.

fig.B./c.4.//II.

fig.B./c.5.//II.

fig.B./c.6.//II.

fig.B./c.7.//II.

fig.B./c.8.//II.


fig.B./c.1.//II.
fig.B./c.2.//II.
fig.B./c.3.//II.
fig.B./c.4.//II.
fig.B./c.5.//II
fig.B./c.6.//II.

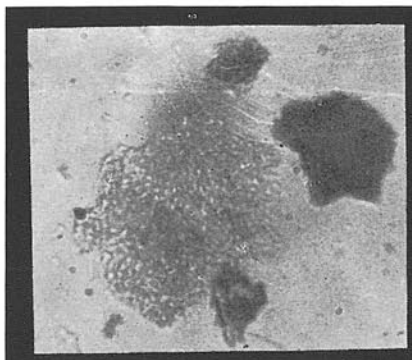

fig.B./c.7.//II

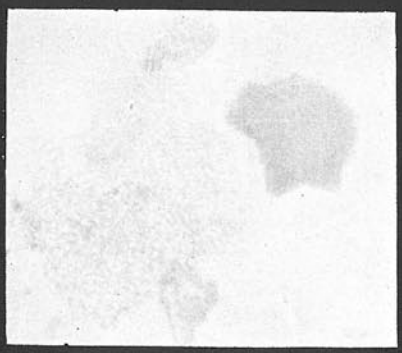

fig.B./c.8.//II.

fig.B./c.9.//II.

fig.B./c.10.//II.

fig.B./c.11.//II.

fig.B./c.12.//II.

fig.B./c.14.//II.

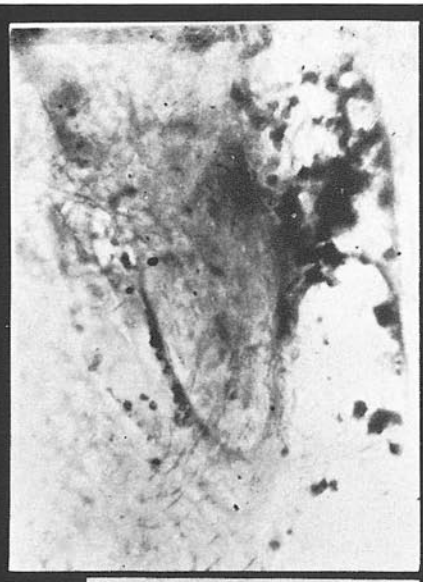

fig.B./c.15.//II.

fig.B./c.16.//II.

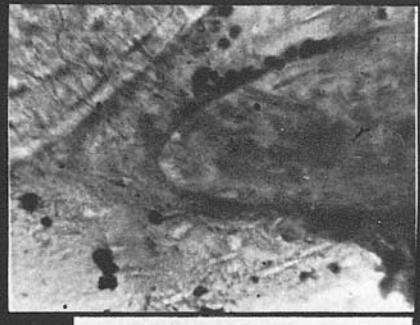

fig.B./c.17.//II.

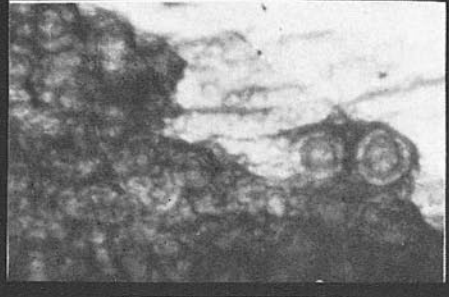

fig.B./c.18.//II.

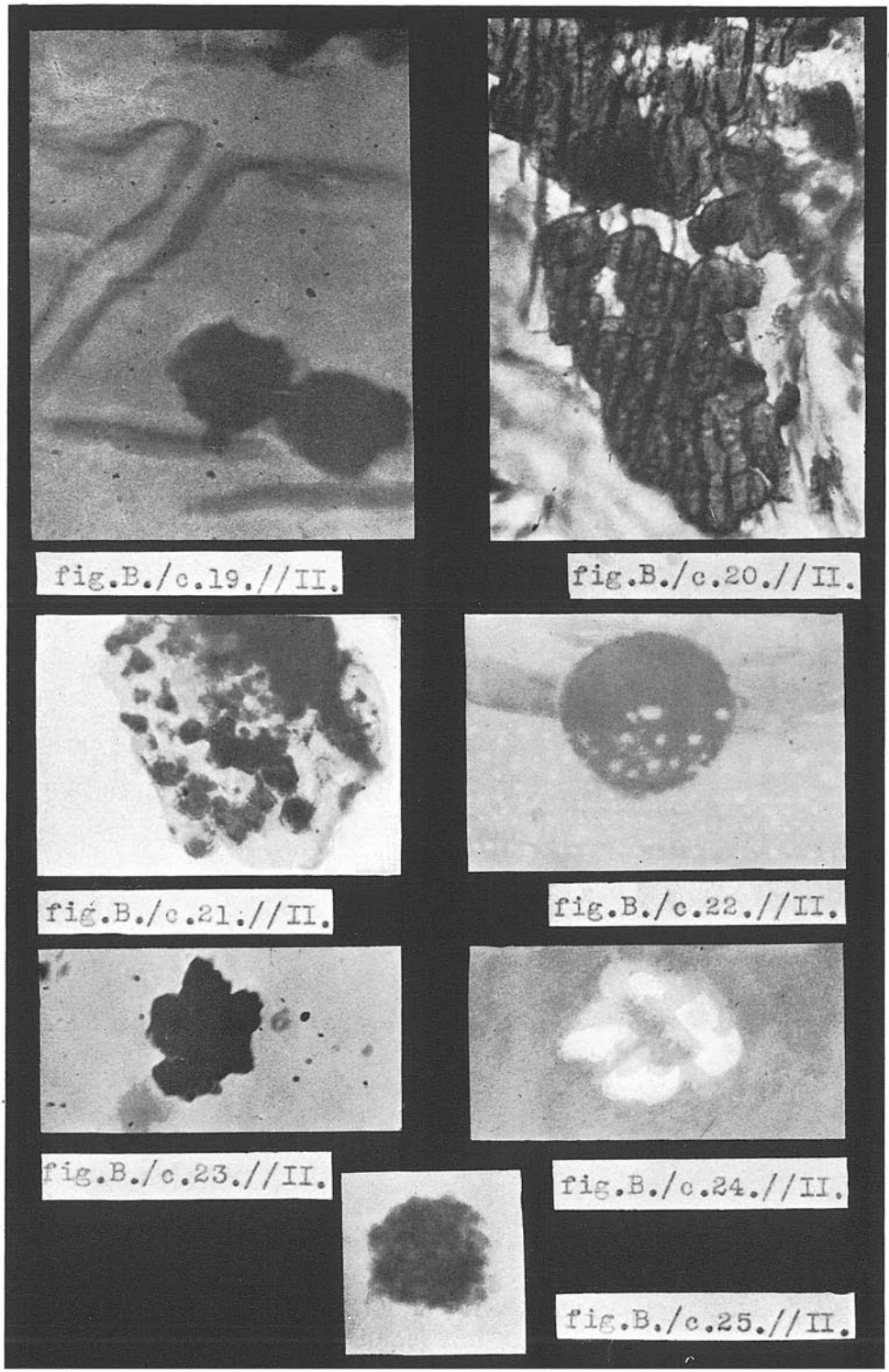

fig.B./c.19.//II.

fig.B./c.20.//II.

fig.B./c.21.//II.

fig.B./c.22.//II.

fig.B./c.23.//II.

fig.B./c.24.//II.

fig.B./c.25.//II.

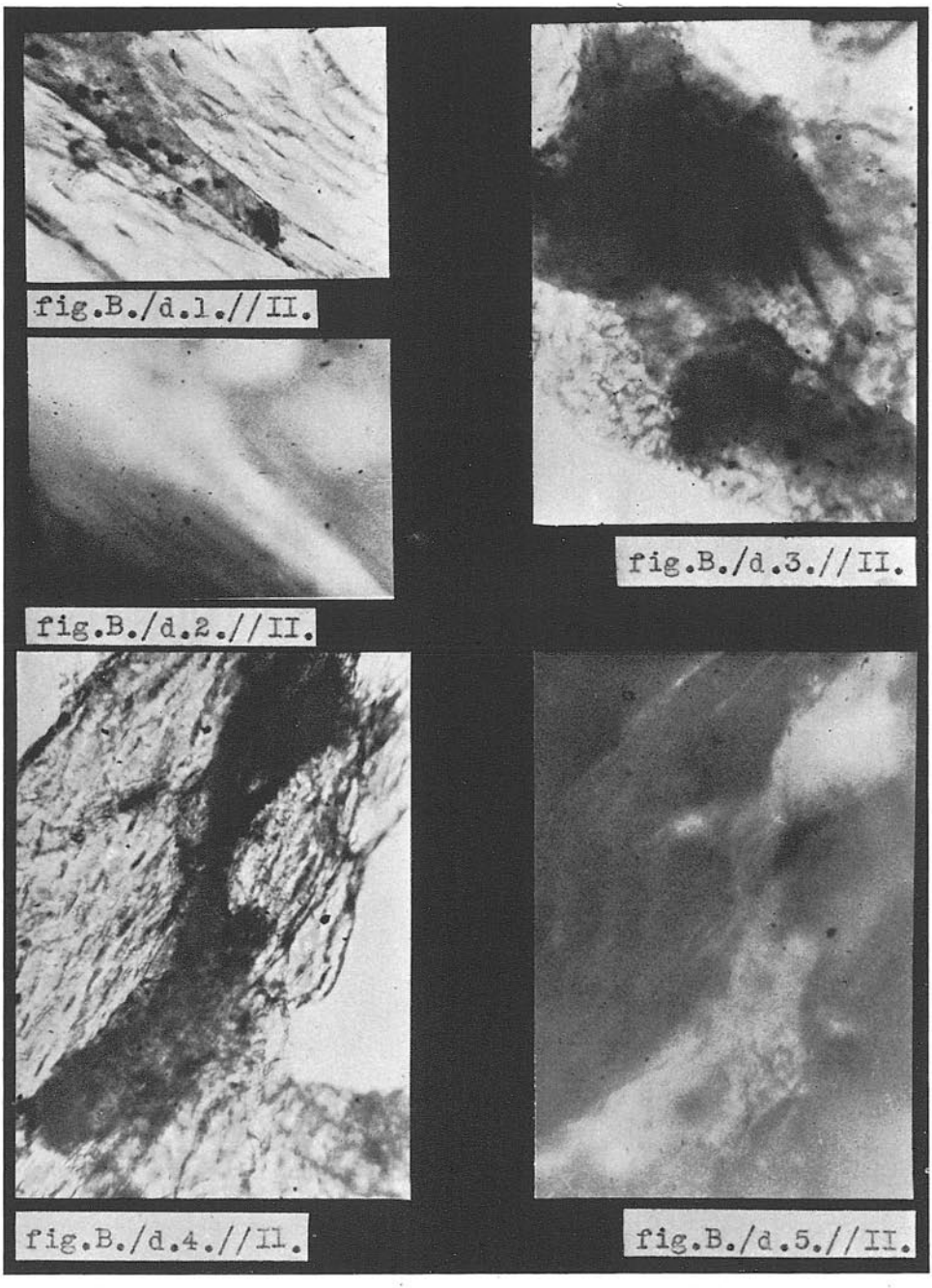

fig.B./d.1.//II.

fig.B./d.2.//II.

fig.B./d.3.//II.

fig.B./d.4.//II.

fig.B./d.5.//II.

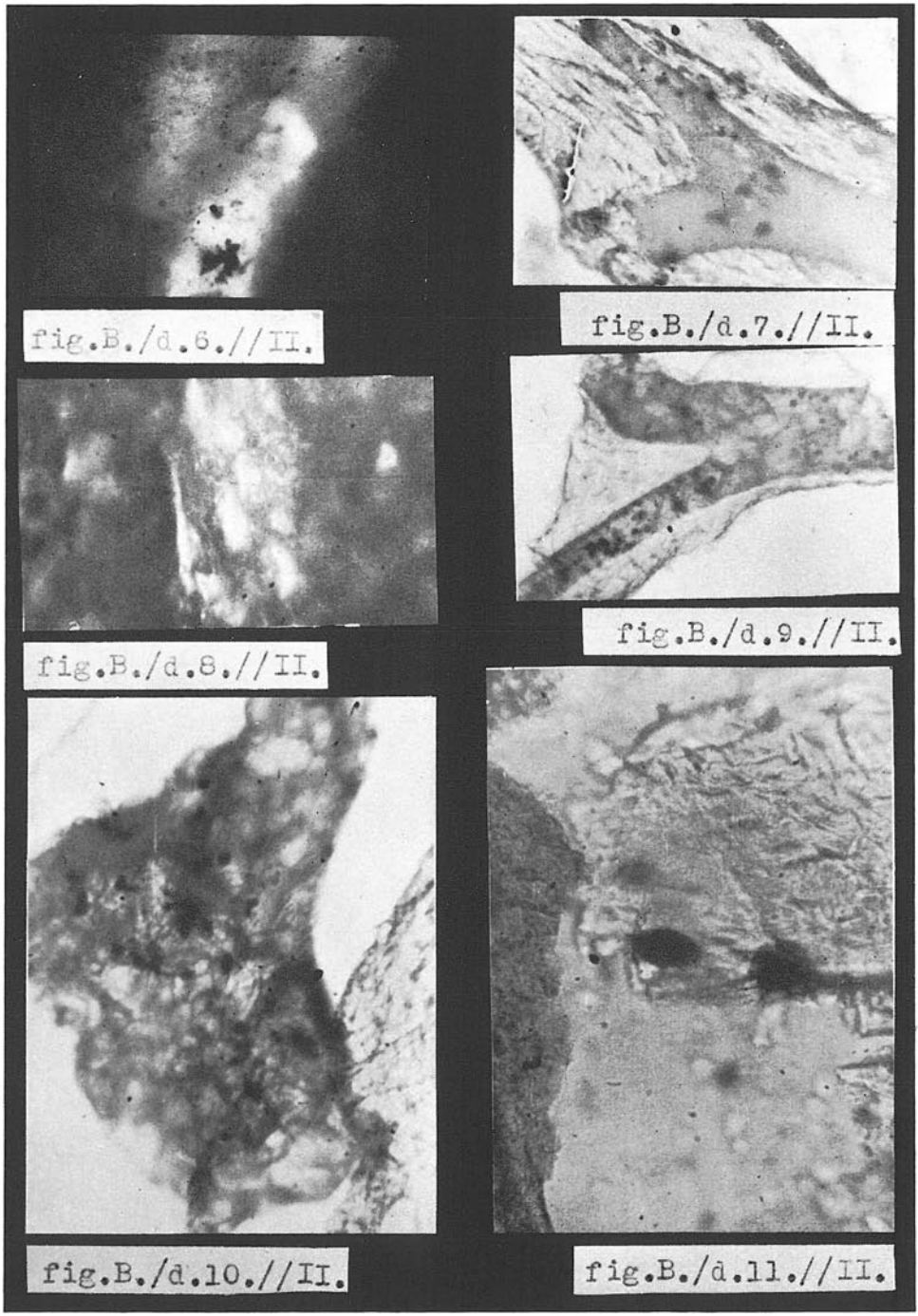

fig.B./d.6.//II.

fig.B./d.7.//II.

fig.B./d.8.//II.

fig.B./d.9.//II.

fig.B./d.10.//II.

fig.B./d.11.//II.

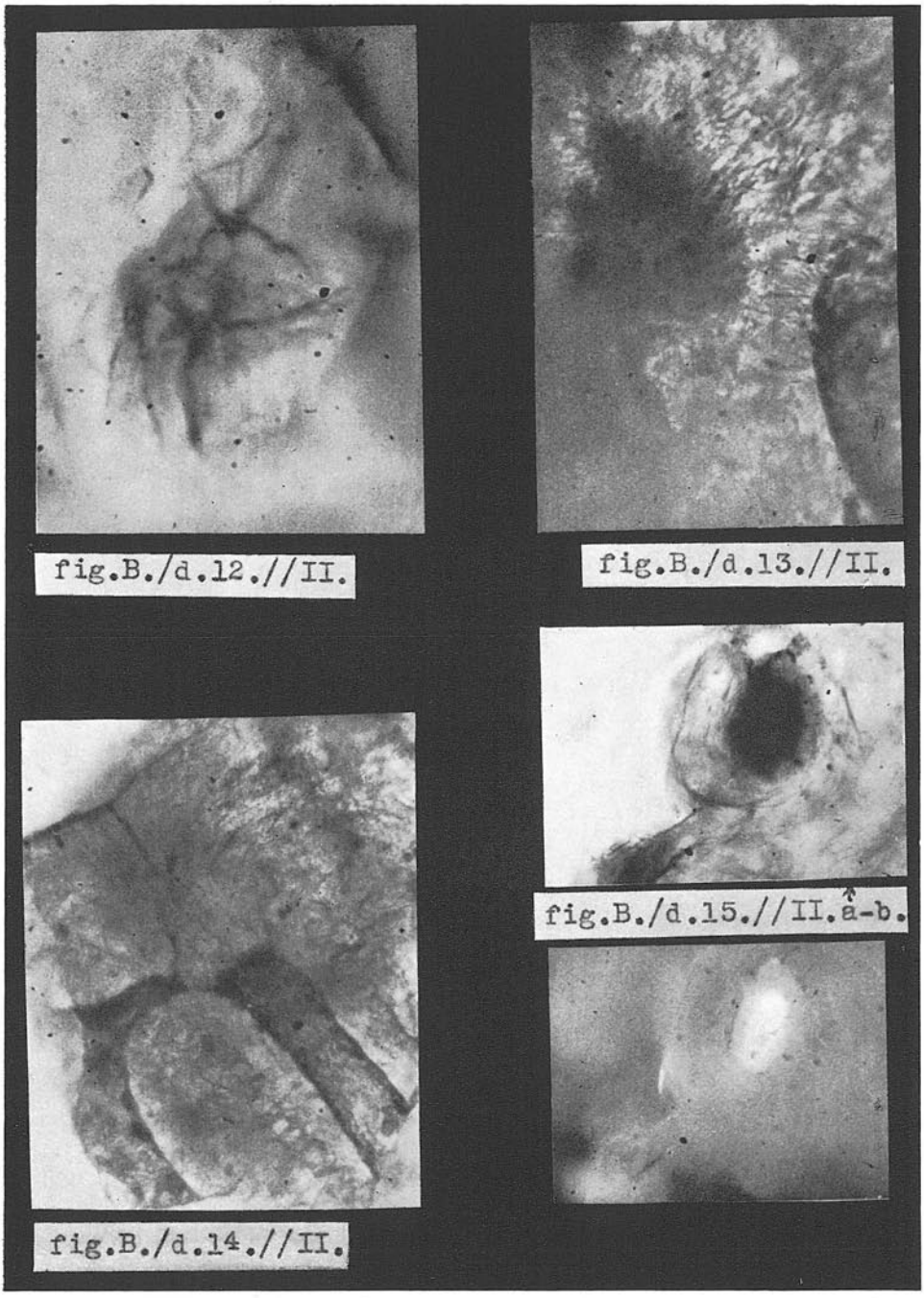

fig.B./d.12.//II.

fig.B./d.13.//II.

fig.B./d.15.//II.a-b.

fig.B./d.14.//II.

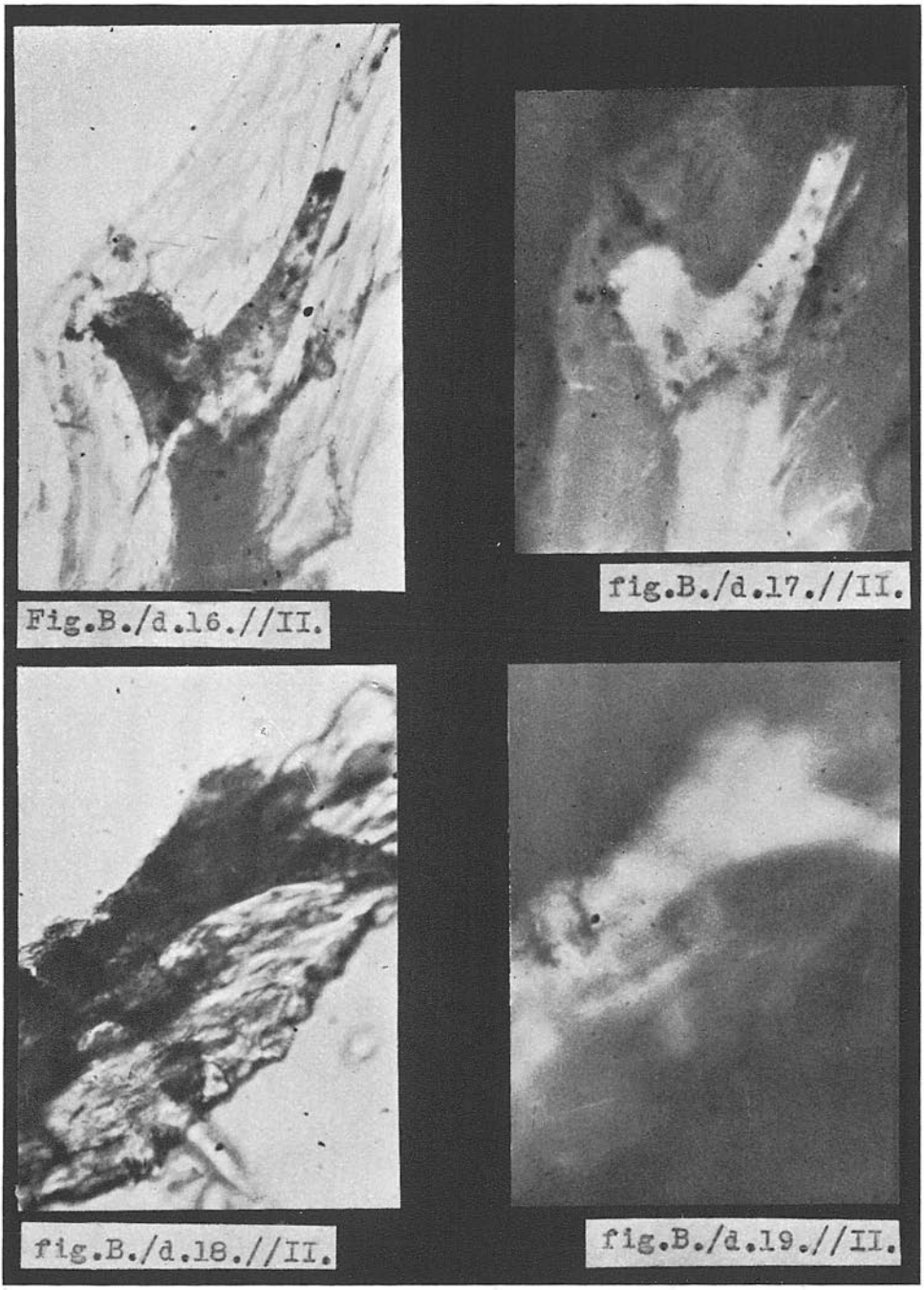

Fig.B./d.16.//II.

fig.B./d.17.//II.

fig.B./d.18.//II.

fig.B./d.19.//II.

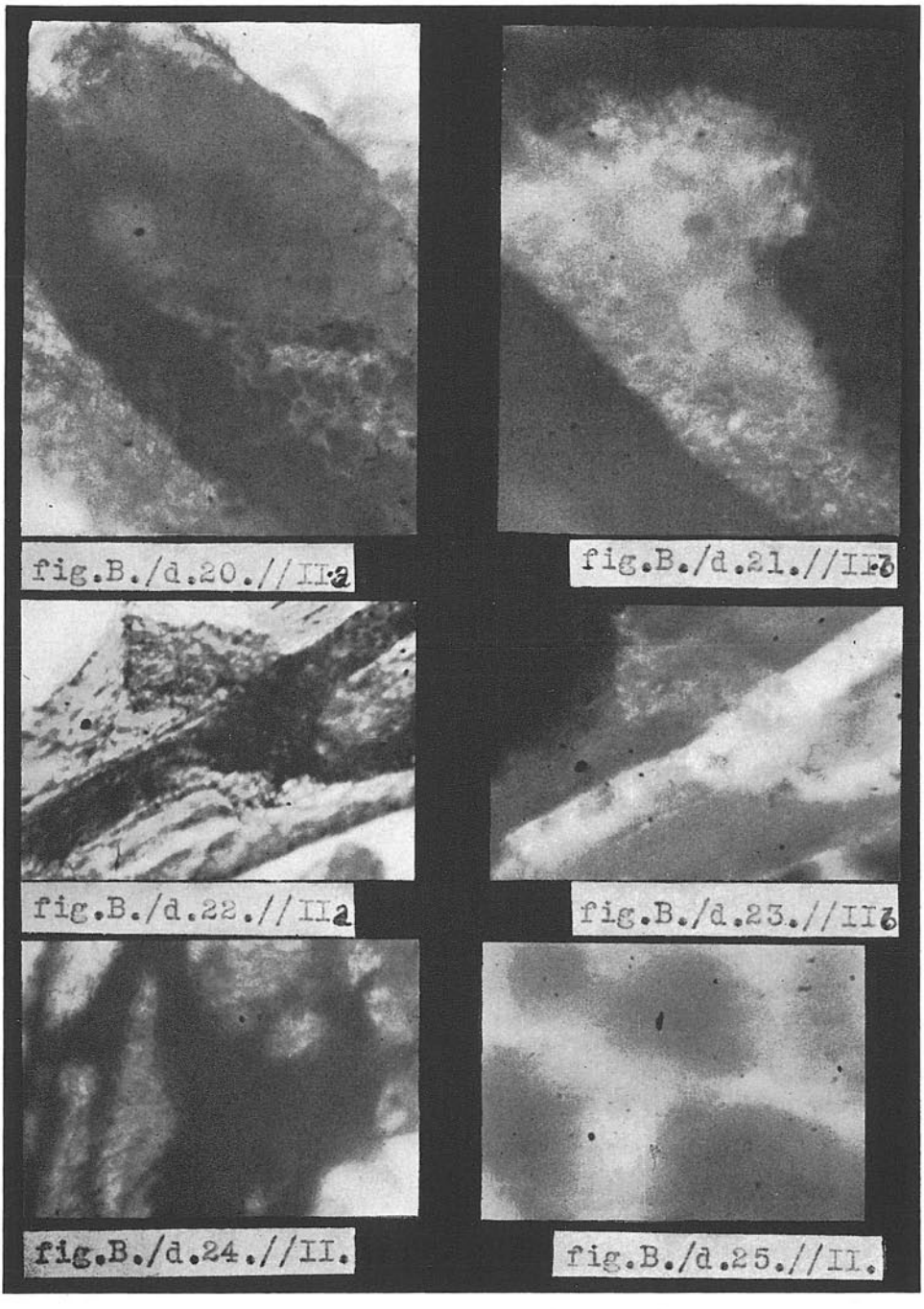
fig.B./d.20.//IIa
fig.B./d.21.//IIb
fig.B./d.22.//IIa
fig.B./d.23.//IIb
fig.B./d.24.//II.
fig.B./d.25.//II.

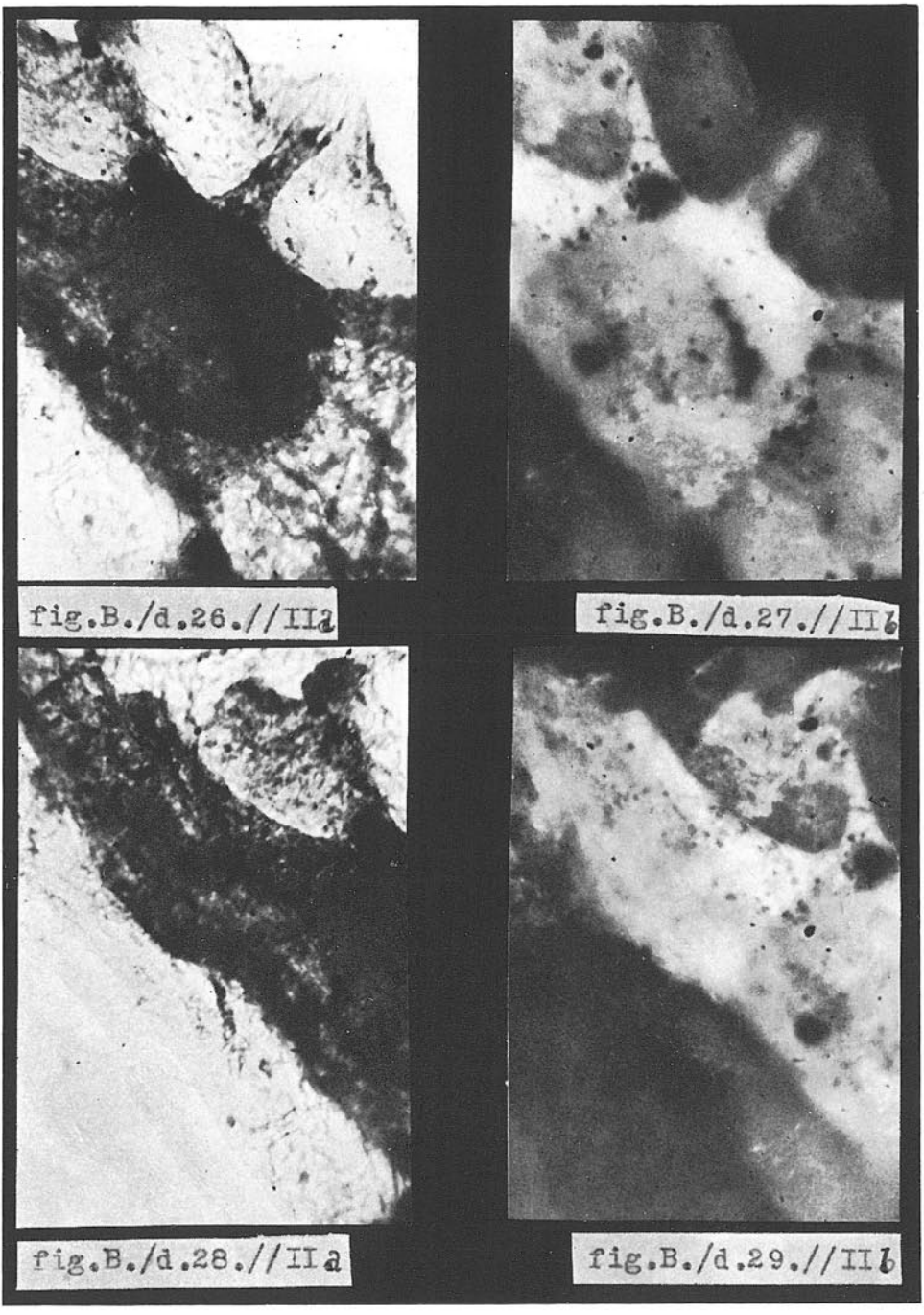

fig.B./d.26.//IIa

fig.B./d.27.//IIb

fig.B./d.28.//IIa

fig.B./d.29.//IIb

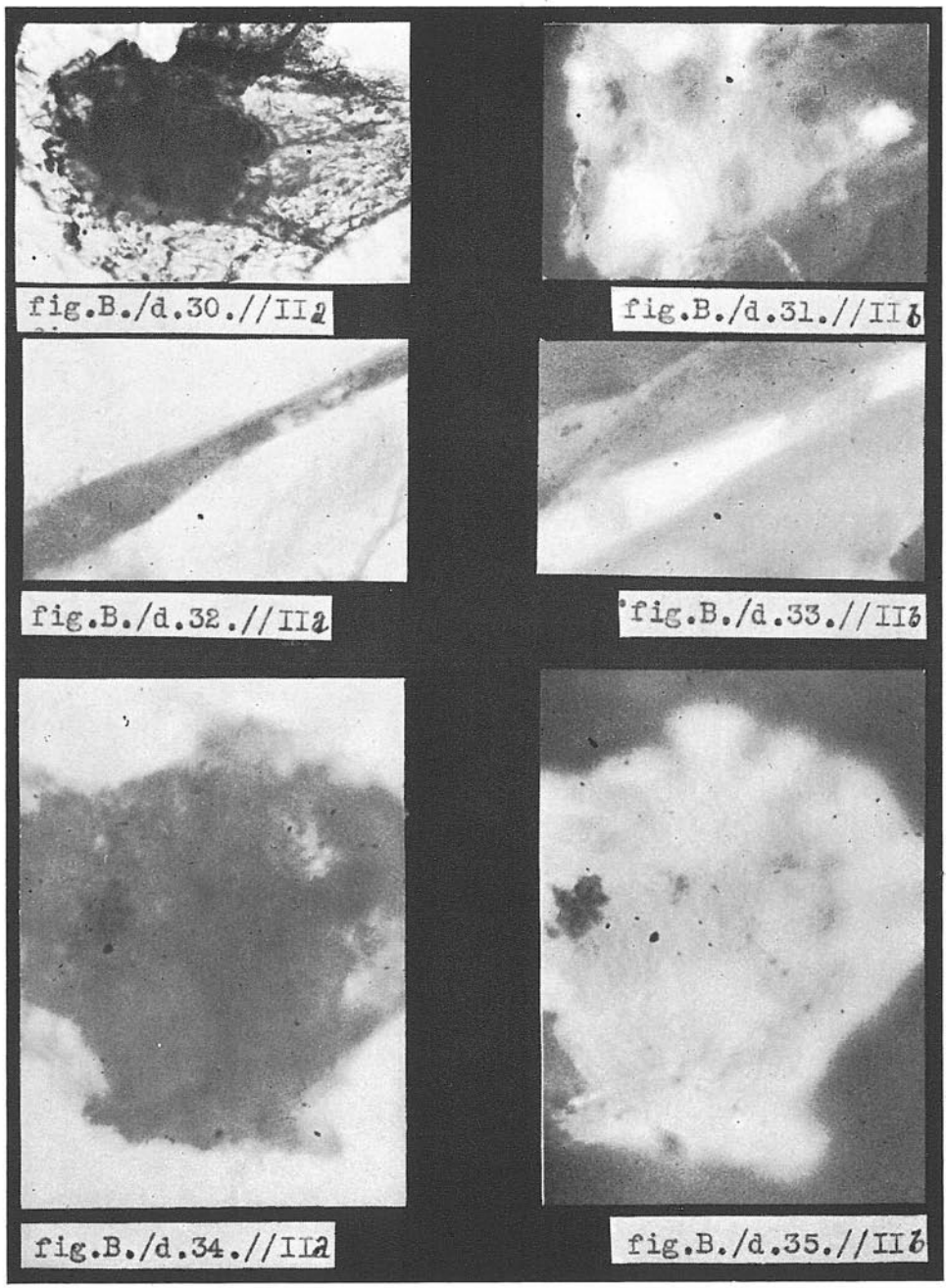
fig.B./d.30.//II2
fig.B./d.31.//II2
fig.B./d.32.//II2
fig.B./d.33.//II3
fig.B./d.34.//II2
fig.B./d.35.//II3

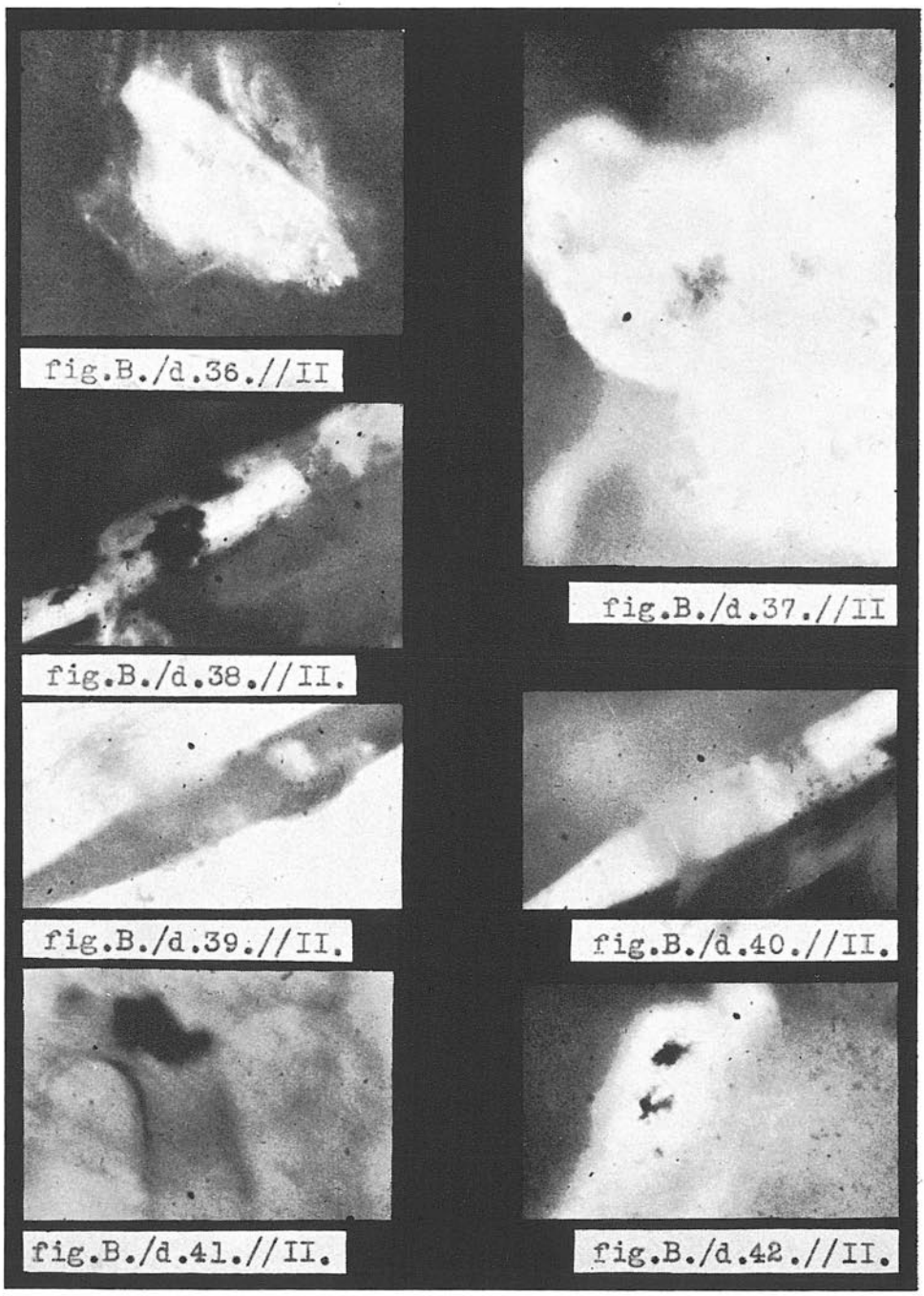

fig.B./d.36.//II

fig.B./d.37.//II

fig.B./d.38.//II.

fig.B./d.39.//II.

fig.B./d.40.//II.

fig.B./d.41.//II.

fig.B./d.42.//II.

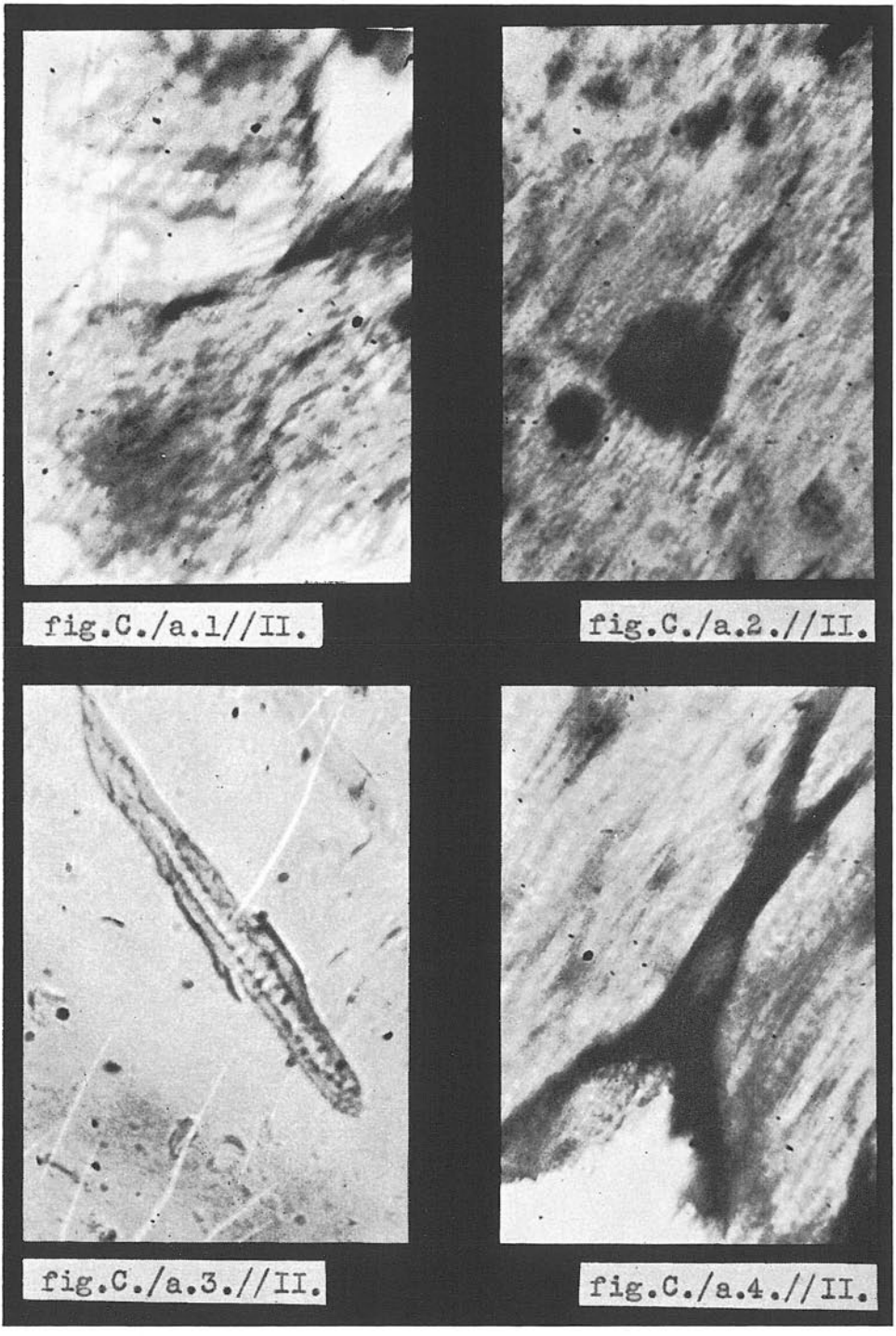
fig.C./a.1//II.
fig.C./a.2.//II.
fig.C./a.3.//II.
fig.C./a.4.//II.

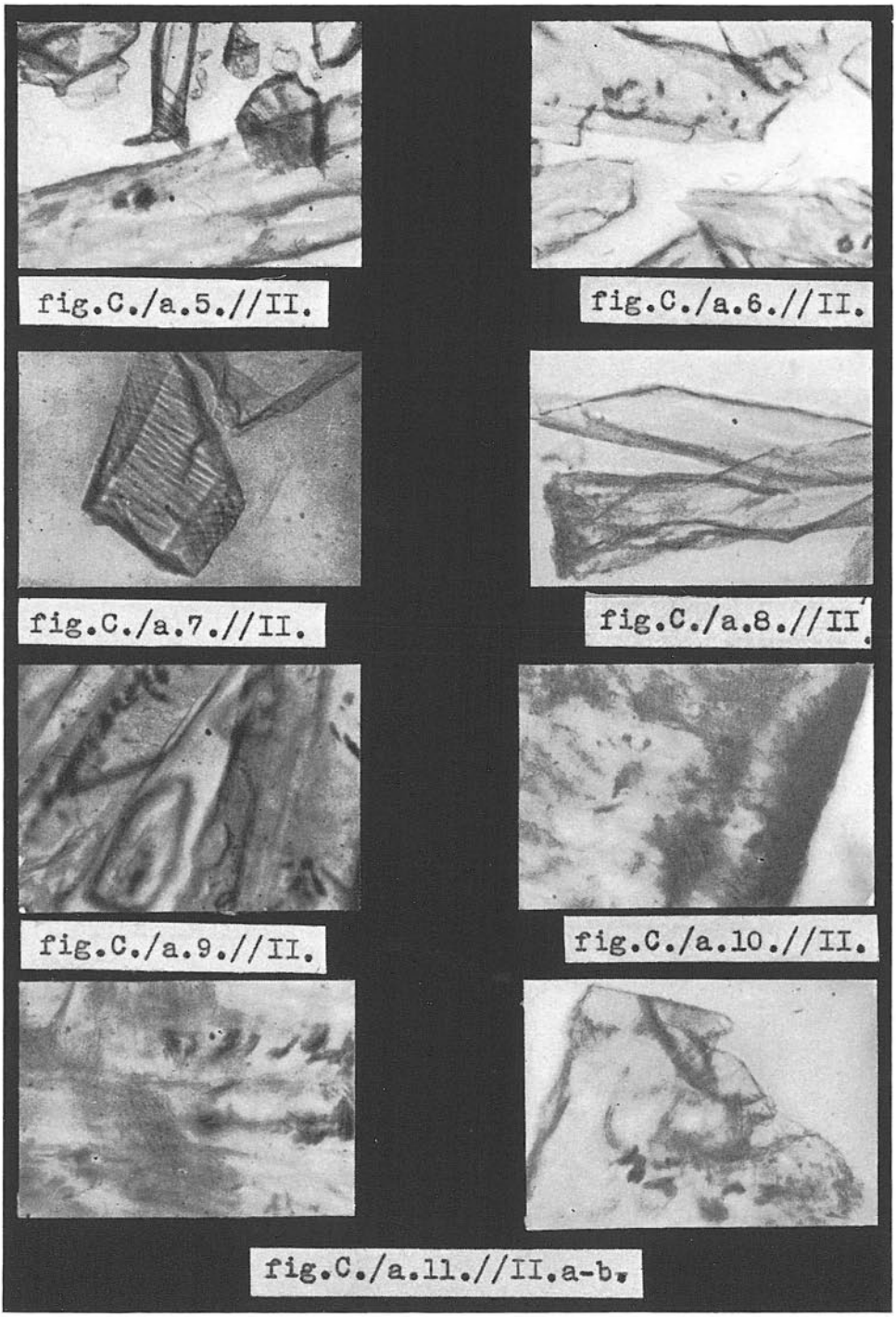

fig.C./a.5.//II.

fig.C./a.6.//II.

fig.C./a.7.//II.

fig.C./a.8.//II.

fig.C./a.9.//II.

fig.C./a.10.//II.

fig.C./a.11.//II.a-b.

fig.C./a.12.//II.

fig.C./a.13.//II.

fig.C./a.14.//II.

fig.C./a.15//II.